ADVANCED SENSOR RESEARCH
Open Access
www.advsensorres.com

Advances in Electrochemical Sensors for Detecting Analytes in Biofluids

*Jimin Lee, Myung Chul Kim, Ira Soltis, Sung Hoon Lee, and Woon-Hong Yeo**

More than half of all Americans suffer from chronic diseases, the leading causes of death and disability. However, prompt treatment of chronic diseases can lead to better patient outcomes and a reduced burden on the healthcare system. This highlights the urgent need for electrochemical (EC) sensors that provide non-invasive, real-time monitoring of disease-indicating biomarkers. Due to their high sensitivity, high selectivity, and cost-effectiveness, EC biosensors have recently shown tremendous promise for individualized health monitoring. This review explains the working principles of EC biosensors. It summarizes the recent advances and improvements of EC biosensors for detecting biomarkers in different biofluids, including tears, saliva, breath, urine, and sweat. Through a comprehensive overview of EC biosensor technologies, this article is expected to aid the development of flexible and wearable EC biosensing systems that have the potential to provide continuous, long-term health monitoring for both clinical and at-home use.

1. Introduction

In the United States, chronic diseases such as diabetes, cardiovascular disease, and stroke are the leading cause of morbidity and mortality, with over 50% of the population afflicted by at least one chronic disease.[1] As a result, the detection, monitoring, and treatment of these diseases are significant objectives of public health activities. Recent advances in medicine have led to a greater understanding of several diseases and their respective therapies. Traditionally, hospitals, specialists, and clinics have used non-invasive but overly technical examination procedures, such as X-ray, magnetic resonance imaging, and radiology computed tomography (CT), or invasive examination procedures, such as blood tests, biopsies, and endoscopies, for medical diagnosis.[2] Conventional invasive procedures rely on incisions and finger pricks to get blood or interstitial fluid, which could be painful and uncomfortable for patients. In addition, the recurrent practice can easily result in infections, particularly in older and diabetic people whose wounds heal slowly.[3] Moreover, they are not appropriate for continuous monitoring of disease diagnostics (e.g., hypoglycemic shock during intense exercise). Using biofluids that are naturally secreted beyond the skin barrier, such as tear, saliva, urine, and perspiration, provides novel, non-invasive detection approaches preferable to conventional procedures. Human biofluids include an excess amount of potentially disease-associated biomarkers, such as electrolytes, nutrients, metabolites, gas molecules, peptides, proteins, and other minute molecules, which facilitate the evaluation of a person's clinical status. These biomarkers should have a possible correlation with their blood equivalent or the disease of interest.[4] Constant monitoring of glucose levels in sweat, for example, facilitates the diagnosis and treatment of metabolic

J. Lee, M. C. Kim, I. Soltis, S. H. Lee, W.-H. Yeo
IEN Center for Human-Centric Interfaces and Engineering
Institute for Electronics and Nanotechnology
Georgia Institute of Technology
Atlanta, GA 30332, USA
E-mail: whyeo@gatech.edu

J. Lee, I. Soltis, W.-H. Yeo
George W. Woodruff School of Mechanical Engineering
College of Engineering
Georgia Institute of Technology
Atlanta, GA 30332, USA

M. C. Kim
Department of Mechanical Engineering
Korea Advanced Institute of Science and Technology
Daejeon 34141, Republic of Korea

S. H. Lee
School of Electrical and Computer Engineering
College of Engineering
Georgia Institute of Technology
Atlanta, GA 30332, USA

W.-H. Yeo
Wallace H. Coulter Department of Biomedical Engineering
Parker H. Petit Institute for Bioengineering and Biosciences, Institute for Materials
Institute for Robotics and Intelligent Machines
Neural Engineering Center
Georgia Institute of Technology
Atlanta, GA 30332, USA

The ORCID identification number(s) for the author(s) of this article can be found under https://doi.org/10.1002/adsr.202200088

DOI: 10.1002/adsr.202200088

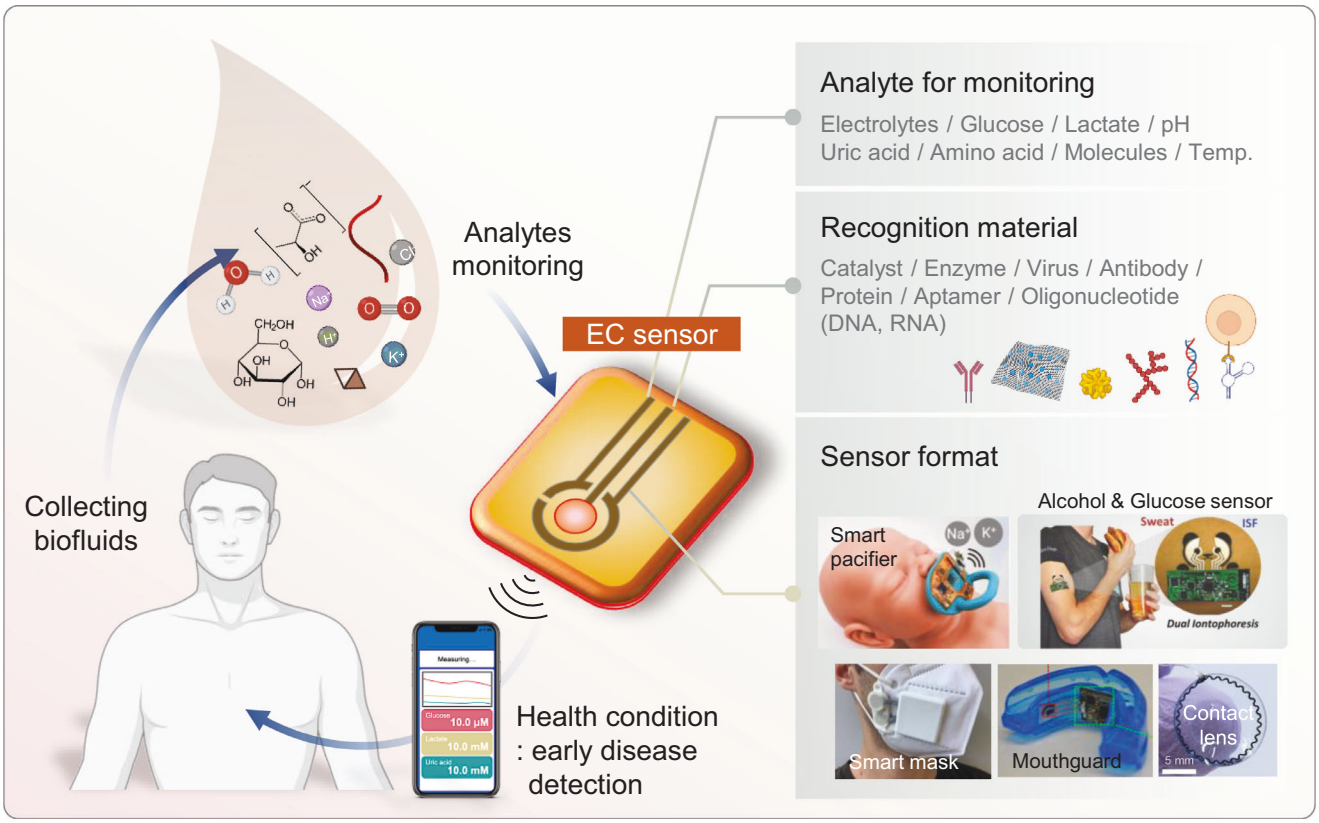

Figure 1. Detection of various analytes with EC sensors from biofluids (e.g., tear, saliva, breath, urine, and sweat) taken from various body positions. (Smart pacifier: Reproduced with permission.[12c] Copyright 2022, Elsevier.), (Alcohol and glucose sensor: Reproduced according to the terms of the CC BY license.[14] Copyright 2018, The authors, published by Wiley VCH), (Smart mask: Reproduced according to the terms of the CC BY license.[15] Copyright 2021, The authors, published by MDPI), (Mouthguard: Reproduced with permission.[16] Copyright 2015, Elsevier), (Contact lens: Reproduced according to the terms of the CC BY license.[12e] Copyright 2021, The authors, published by Springer Nature).

diseases like diabetes. By continually detecting the level of these biomarkers, patients have access to simple self-measurement, self-monitoring, and comprehensive feedback on their health status. This marked the beginning of the era of diagnostics at the point of care and remote disease monitoring. These improvements are especially beneficial to elderly individuals living at home and critically ill patients, allowing them and their caregivers to monitor their health status and the development of variables impacting their health continuously and easily. Health monitoring needs a sensing system, which should be a highly sensitive, robust, portable, and inexpensive biosensor that can detect the main analytes and pathogens/cells in biofluids. This will improve the current healthcare system by bringing diagnostic tools closer to the patient and allowing for faster and more frequent remote checkups. Electrochemical (EC) sensors are the most common analyte detection method due to their high accuracy, high sensitivity, fast response time, potential for miniaturization, and potential for continuous monitoring.[5] EC sensors typically target a single analyte and the main EC analytes are electrolytes, glucose, pH, and lactic acid.[1b,5,6] In recent years, there has been a growing trend toward making multivariate sensing systems on a single chip.[7] Such sensing systems are being integrated into flexible and wearable continuous monitoring devices that can wirelessly connect to smartphones and other compatible electronic devices to display and share relevant data and diagnostics.[8] This data can be used for medical applications like early detection of diseases, monitoring of disease progression, and development of treatment plans. Additional applications include fitness tracking, sports science, and monitoring the overall status of the body.[9] Overall, this review offers a selection of recent articles devoted to the development of EC sensors for various biofluid sensing applications and the current advancements in EC sensor selectivity, sensitivity, and long-term stability. Several views addressing the future development and direction of EC sensors in health applications are also presented.

2. Electrochemical Sensors for Detecting Analytes in Various Biofluids

2.1. Basic Concepts of Electrochemical Sensors

Generally, EC sensing is best understood as a series of three procedures: Recognition of a target analyte, transduction, and signal output.[10] **Figure 1** shows an overview of the analyte detection procedure using human biofluids. Catalysts and enzymes on electrodes are commonly used to recognize the analytes in biofluids. The electrode or transducer converts the detected analyte into a proportional electrical signal that can be measured.

The electrode or transducer converts the detected analyte into a proportional electrical signal that can be measured.[11] For example, an enzymatic sensor has enzymes immobilized on the electrode surface. When the sensor is exposed to a solution, having a certain concentration of the target analyte, the sensor electrochemically reacts (involving electron transfers) with the analyte, making a measurable electrical signal that can include current, resistance, or potential changes. By using the proper transducer, the difference in the analyte concentration can be converted into a measurable electrical signal and sent to a digital device for data storage and display. EC sensors can be provided in a variety of form factors including fully integrated wearable devices, such as an ultrathin microfluidic patch for sweat monitoring, a pacifier, mask, contact lens, or on-tooth patch.[12] Commonly, a three-electrode configuration is employed in EC sensing: The working electrode (WE), the reference electrode (RE), and the counter electrode (CE; also known as an auxiliary electrode). The WE has an electroactive layer (e.g., catalyst) or bioactive material (e.g., enzymes, antibodies) on the surface to promote the redox or biochemical reaction of interest. Thus, the type of active material, its microstructure, and its dimensions greatly influence the detection ability.[13] The RE, which is most often made from Ag/AgCl, maintains a constant and stable potential during such EC reactions. The CE is often used to establish the connection to the electrolytic solution so that a current can be applied to the WE and is made from a stable and inert conducting substance (e.g., platinum, gold, or carbon—depending on either analyte or environmental condition). The following sections examine the relationship between distinct classes of analytes and detection mechanisms. Based on its operating principle, the EC sensor can be categorized as an amperometric, potentiometric, impedimetric, or voltammetric sensor. When selecting the optimal techniques for detecting the target analyte, the suitable operating mechanism must be considered.

2.1.1. Working Principles

Potentiometric Sensors: The measurement is performed in "open circuit" (i.e., zero-current) conditions with a two-electrode setup. Since there is only a voltage measurement, there is no need for a power source. The voltage across WE and RE is measured with a high-input impedance voltmeter, to minimize the contribution of the ohmic potential drop to the total difference in potential. The potential of WE, thanks to an accumulation of charged molecules (ions), exclusively depends on the analytical concentration of the analyte in biofluids, while the RE is needed to provide a defined reference potential.[17] Ion-selective electrodes (ISEs), coated-wire electrodes, and field-effect transistors are examples of potentiometric EC sensors. For example, ISEs have been leveraged for monitoring of electrolytes (e.g., Na^+, K^+, Cl^-, or Ca^{2+}).[18] The potentiometric sensor is also widely employed in the monitoring of pH levels.[19] Without the need for costly, complex measurement equipment, potentiometric sensors have shorter development times, higher sample rates, are more durable, and are readily applicable for miniaturized monitoring devices.[20]

Amperometric Sensors: In amperometry, electrocatalytic redox reactions are triggered by a constant applied voltage between the WE and RE, and the resulting electrical current is proportional to the concentration of the analyte being measured. The WE potential is set to a fixed value by a voltage supply, and the current produced by electroactive molecules undergoing electron transfer with the WE is measured in a three-electrode system.[20] The amperometric sensor can detect a wide variety of biomarkers, including glucose, lactate, and tiny gas molecules (e.g., alcohol and oxygen).[21]

Voltammetric Sensors: A voltammetric sensor measures a produced current between the WE and CE upon sweeping a potential between the WE and RE, where the measured current is consequence of the electrochemical reaction (e.g., oxidation, reduction) between the electroactive recognition elements and the target analyte on the surface of WE. Current responses are often recorded as a peak, which corresponds to the electroactive species concentration.[5]

Impedimetric Sensors: The working principle of impedimetric sensors is that a recognition element (e.g., proteins) coupled to the conductive surface of WE, behaves as an insulator and chemical bonds between the recognition material and target analytes (e.g., antibody-antigen binding) result in a change in an impedance that depends on target analyte concentration.[22] Impedimetric sensors can provide signal changes even if there is no electroactivity during a reaction between the recognizing element and the analyte of interest. The use of low voltage is one of the most significant benefits of impedimetric EC sensors, enabling ideal detection of the analytes without significantly altering the ionic balance. In contrast, amperometric and voltametric EC sensors need an applied external voltage to induce a redox reaction.[20]

Conductometric Sensors: Conductometric sensors quantify the change in the conductance between the pair of electrodes, where the conductivity of the analyte is variable as the EC reaction proceeds. In other words, conductivity is proportional to target analyte concentration. This type of sensor is usually used to monitor metabolic processes in living biological systems.[23]

2.2. Detectable Analytes in Biofluids

Biofluids are promising candidates for non-invasive detection by a variety of sensor platforms and analyte monitoring can be performed on various body sites for different physiological biomarkers (**Figure 2**).[24] The potential analytes found in various biofluids, along with their reported normal concentration ranges, related human health status, and potential diagnostic applications are discussed in the following sections and listed in **Table 1**.

2.2.1. pH

pH regulation is one of the most important functions of homeostasis because pH directly affects all biological processes. Thus, monitoring pH can indicate problems with homeostasis that can have adverse medical effects.[5,41] For example, acidosis can cause headache, lethargy, or fatigue, while alkalosis can cause cognitive impairment, tingling or numbness in the extremities, muscle twitching and spasm, and nausea and vomiting. In addition, abnormal sweat pH reflects skin lesions such as irritant contact dermatitis, acne, and atopic dermatitis.[42] Many cellular processes and enzymatic reactions also depend on pH, and low pH of

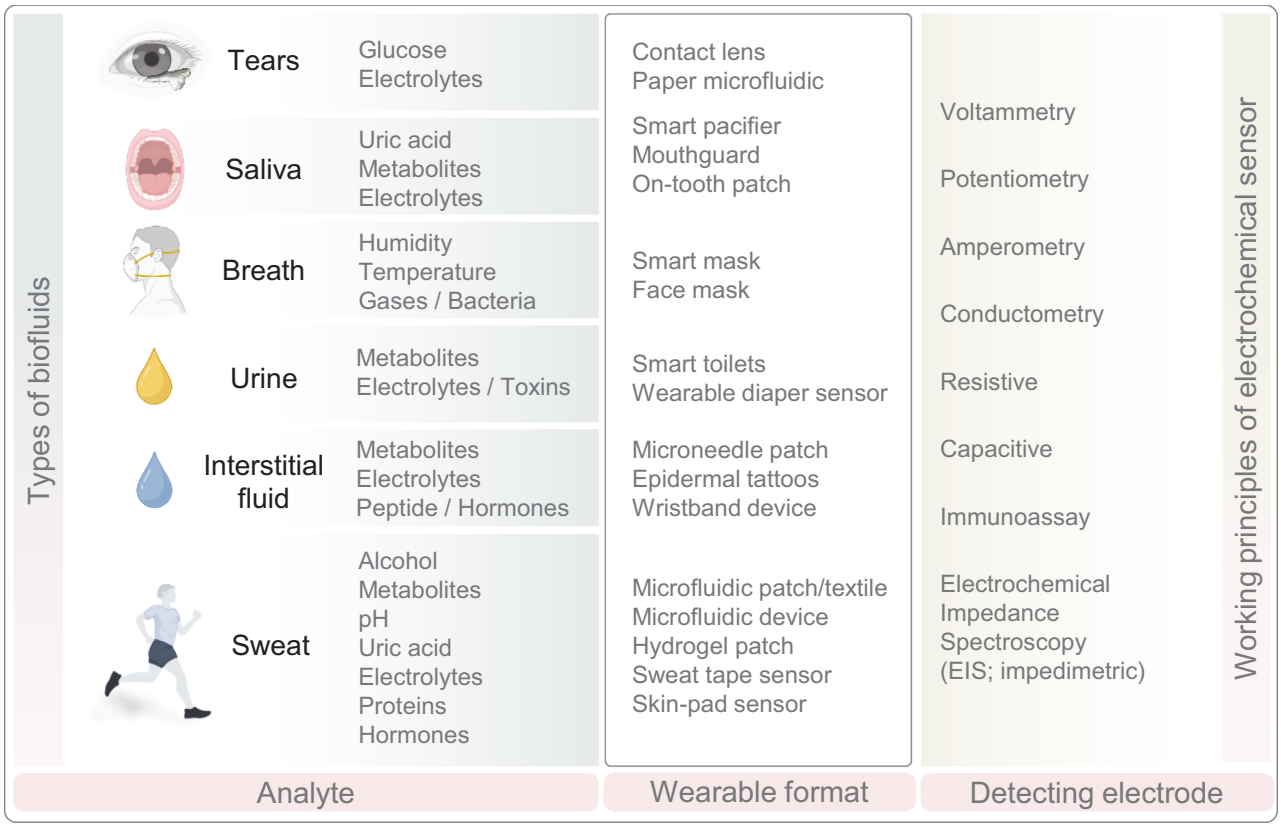

Figure 2. Analytes in various biofluids, target applications, and working principles of electrochemical sensors.

biofluid (≈6.5) suggests the destruction of living cells and the promotion of tumorigenesis. It is reported that acidic environments inflame blood cells, lower oxygen levels, impair cell metabolism, and disrupt the function of DNA and respiratory enzymes, leading to kidney, liver, and sweat gland malfunction.[43]

2.2.2. Electrolytes

Electrolytes are regarded as one of the most essential molecules for maintaining the fluid equilibrium of cells. At present, the reported entities that can be detected by EC sensors involve multiple species, such as pH, Na^+, K^+, Ca^{2+}, NH_4^+, Cl^-, etc.[44] The most important electrolytes are sodium (Na^+), potassium (K^+), and chloride (Cl^-) ions. These ions contribute to neuronal excitability, endocrine secretion, membrane permeability, buffering of bodily fluids, and movement regulation of fluid flow.[45] For example, Na^+ helps with intracellular liquid volume regulation, nerve and muscle function, and acid–base balance. Seizures or coma may result from hyponatremia accompanied by an aberrant Na^+ deficiency. K^+ cooperates with Na^+ on the fluid balance and acid–base balance, while Ca^{2+} is essential for muscle contraction, enzyme activity, and blood coagulation.

2.2.3. Metabolites (Glucose, Lactate, Uric Acid)

As aforementioned, the number of diabetic patients who are suffering from glucose dysregulation has rapidly increased during the last decade.[46] Therefore, glucose level monitoring has been regarded as an important health indicator. As a result, the function of glucose concentration sensing has been embedded into many recent flexible and wearable sensors for biofluid monitoring.[47] Monitoring lactate levels in the body is crucial for clinical diagnosis related to the anaerobic metabolic pathways since elevated lactate concentrations can lead to respiratory or hepatic failure, as well as, sickness and physiological weariness. Serious ailments such as pyruvate metabolism problems, meningitis, heart failure, liver disease, sepsis, and tissue hypoxia may result from elevated lactate levels.[48] Uric acid (UA) is the result of purine metabolic oxidation in the human body. If the UA level is abnormally increased due to impaired renal excretion or various risk factors such as increased consumption of purines and alcohol, UA can accumulate in the body resulting in type 2 diabetes. Consequently, monitoring UA in biofluids is imperative for diagnosing certain disorders, such as renal syndrome, and gout, and managing urate-lowering therapy, flare-up prevention, and dietary or nutritional control.[49] EC sensors for metabolite monitoring can be categorized into two groups: Enzymatic sensors, where the metabolites are detected indirectly through hydrogen peroxide molecules (H_2O_2) production, and non-enzymatic sensors (also known as enzymatic-free sensors) with a catalyst, where the change in the physical properties including an electron transfer is used for analyte detection.[50] The enzymatic sensor incorporates a multilayered structure that consists of the metabolite-permeable polymeric layer, the enzyme-immobilized layer, and hydrogen peroxide (H_2O_2)-permeable layer, because H_2O_2 is a

Table 1. Important analytes and their typical concentrations in tear and saliva.

Biofluid	Analyte	Concentration range	Reflecting human health status and diagnostic application	Ref.
Tear	Na^+	120–165 mM	Cystic fibrosis, muscle cramp, hyper/hyponatremia	[25]
	K^+	20–42 mM	Hyper/hypokalemia and an indicator of ocular disease	[26]
	Cl^-	118–135 mM	Cystic fibrosis, lung disease, hyper/hypochloremia, and potentially for hydration status and electrolyte stores	[27]
	Glucose	0.013–0.051 mM; <0.6 mM	Diabetes management, metabolic syndrome	[28, 29]
	Lactate	2.0–5.0 mM	Fatigue level, lactic acidosis, ischemia, sepsis, liver disease and cancer, hydration plan	[30]
	Urea	3.0–6.0 mM	Renal function, metabolism status	[31]
	Uric acid	25–150 μM	Gout, arthritis, heart disease diabetes, cardiovascular diseases	[32]
	Lactoferrin	≈2.2 mg mL^{-1}	Diagnosis of severe dry eye disease	[33]
	Ascorbic acid	3.9–23 mg dL^{-1}; 220–1310 μM	Detection of eye trauma, cornea inflammation	[34]
	Cortisol	1–40 ng mL^{-1}	Psychological stress (anxiety), stress disorder, Cushing syndrome, Addison's disease	[35]
	Dopamine	0.37 mM	Glaucoma	[36]
	Pyruvate	0.05–0.35 mM	Genetic disorders of mitochondrial energy metabolism	[37]
Saliva	pH (H^+)	6.6–7.1	Acidosis and alkalosis, muscle spasms, nausea, vomiting, numbness in face, feet, or hands	[38]
	Na^+	4–37 mM	Cystic fibrosis, muscle cramp, hyper/hyponatremia	[12c]
	K^+	2.6–18.3 mM	Hyper/hypokalemia and an indicator of ocular disease	[12c]
	Cl^-	7–18 mM	Cystic fibrosis, lung disease, hyper/hypochloremia, and potentially for hydration status and electrolyte stores	[39]
	Glucose	0.233–1.776 mM	Diabetes management, metabolic syndrome	[40]
	Lactate	0.11–0.56 mM	Fatigue level, lactic acidosis, ischemia, sepsis, liver disease and cancer, hydration plan	[16]
	Uric acid	100–250 μM	Gout, arthritis, heart disease diabetes, cardiovascular diseases	[16]

product of the enzymatic reaction.[51] For example, enzymatic glucose sensing involves the transfer of electrons because of oxidation events between glucose oxidase (GO_x) and glucose. GO_x is a typical flavin enzyme that contains the redox-active cofactor flavin adenine dinucleotide (FAD) and catalyzes the conversion of glucose to gluconolactone.[52] During the reaction, GO_x (FAD) is transformed to GO_x ($FADH_2$), leading to current or voltage changes of the EC sensor. The standard reaction equation can be shown in Equation (1).[53] If there is a presence of oxygen (O_2) introduced, GO_x can produce gluconolactone (Equation (2)), as the glucose is hydrolyzed to gluconic acid and H_2O_2:

$$\text{Glucose} + GO_x\,(\text{FAD}) \rightarrow \text{Gluconolactone} + GO_x\left(FADH_2\right) \quad (1)$$

$$\text{Glucose} + O_2 \xrightarrow{GO_x} H_2O_2 + \text{Gluconic acid} \quad (2)$$

In both processes, enzymes are consumed rather than regenerated, deteriorating sensor stability. The same working principle is used for the detection of lactate and uric acid with lactate oxidase (LO_x) and uricase (UO_x), respectively. Since the enzymatic sensors produce H_2O_2, the oxidation or reduction of H_2O_2 can be used as a sensing mechanism. One area of further improvement for the enzymatic sensors is surface modification of WE (e.g., microstructural modification of polymeric layer, partial functionalization of each layer), which can lower the response time of the EC sensor.[54] In contrast to enzymatic sensors, typical non-enzymatic sensors use a metal oxide (e.g., CuO, NiFe oxides, NiCo-layered double hydroxide (NiCo-LDH)) or combined noble metal and carbon structure to serve as an electrocatalyst for electron transfer during the glucose oxidation reaction.[55] As the catalytic material reacts with glucose, electrons are transferred by electro-oxidation and reduction reactions. In this case, the glucose selectivity of these non-enzymatic sensors depends on the magnitude of the glucose oxidation process; this behavior was initially seen in acidic solutions because pH level influences the degree of catalytic activity.[56]

2.2.4. Gas Molecules

The measurement of nitric oxide (NO) levels or its associated products (e.g., NO_2 and NO_3), particularly in breath, can provide an understanding of several biological processes and medical conditions. In the case of asthmatic patients, there is a generation of NO by inflammatory cells. NO levels in breath range from low to around 100 ppb. Monitoring of ammonia (NH_3) is also useful for a diagnosis of hemodialysis, asthma evaluation, hepatic encephalography, and halitosis analysis. As NH_3 diffuses from the blood into the lungs, it can be detected during a non-invasive breath monitoring.[57] If the gas is detected in the breath, it can be exploited as a diagnostic test for helicobacter pylori stomach disease since excess urea is transformed into NH_3 and bicarbonate in the acidic stomach environment.[58] Increased acetone levels

Table 2. Summary of EC sensors targeting analytes in tear.

Target analyte	Detection method	Recognition material	Linear detection range	Limit of detection	Ref.
Glucose	Amperometry	Enzyme; GO_x	10^{-3}–10 mM	1 μM	[28]
	Amperometry	Enzyme; GO_x	0.1–0.6 mM	0.01 mM	[62]
	Amperometry	Enzyme; GO_x	0–50 mg dL^{-1}	5 mg dL^{-1}	[63]
	Amperometry	Enzyme; GO_x	≈12 mM	9.5 μM	[72]
	Resistive	Enzyme; GO_x	12.6 μM–1 mM	12.6 μM	[73]
	Solution-gated graphene transistor	Enzyme; GO_x	0.01–0.3 mM	0.1 μM	[74]
Uric acid	Solution-gated graphene transistor	Bovine serum albumin-chitosan	0.0003–0.003 mM	0.1 μM	[74]

in the breath are symptomatic of systemic ketosis, which may be caused by the conversion of fat to ketones. This pertains to people with Alzheimer's disease and children getting treatment for seizure control. In addition, abnormal acetone levels in diabetic individuals may signal hypoglycemia, implying the importance of non-invasive monitoring techniques for such diseases by using an EC sensor.[55b]

2.2.5. Body Temperature and Humidity

Temperature is an important indicator of human body health. Several abnormal physiological conditions, including infection and heat can cause fever. Humidity is another important indicator for physiological monitoring. The exhaled nasal air contains more moisture than the inhaled air. By measuring the relative humidity of the air surrounding the nose, we may assess if a person is breathing normally, which may be associated with respiratory and lung conditions such as asthma, chronic obstructive pulmonary disease, lung cancer, etc. The most popular working mechanism for temperature or humidity detection is based on resistive change, in which physical stimuli cause resistance or conductance changes in the sensor.[59]

2.2.6. Electrochemical Sensors Targeting Tear and Saliva

The mainly detectible analytes and corresponding potential diseases, and a summary of the state-of-the-art EC sensor performances are summarized in Tables 1 and **2**, respectively. Tears are an extracellular fluid composed of electrolytes, proteins, peptides, and some metabolites obtained from glands (e.g., lacrimal glands, ocular surface epithelial cells, and goblet cells).[60] In general, there is a difference in the fluid composition between tears and blood. But interestingly, blood fed to the brain can supply the leakage of blood metabolites into the tears. Given that fact, blood-tear correlations served as the basis for the creation of tear proxies capable of simulating the blood levels of certain metabolites. Contact lenses in direct touch with tears can be functionalized or coupled to tiny sensors for continuous diagnostic monitoring of metabolites (e.g., glaucoma monitoring).[61] Recent advances in transparent electrodes, wireless communication technologies, and biosensors have accelerated the development of intelligent contact lenses. Google and Novartis conducted substantial research to develop intelligent contact lenses that can be remotely controlled and provide continuous tear glucose readings. Similarly, Yao et al. produced PET contact lenses for continuous glucose monitoring using a three-electrode EC sensor.[62] Photoresist and thermal evaporation of titanium, palladium, and platinum on a PET coated wafer was used to create the electrodes. The immobilization of glucose oxidase was achieved by covering the contact lens surface with titanium oxide, which also functioned as a passivation layer. Potential interferences from urea, ascorbic acid, and lactate were minimized by using Nafion film. Keum et al. proposed soft contact lenses for simultaneous glucose testing and insulin delivery (**Figure 3**A-a).[63] The ultrathin flexible electrical circuit, microcontroller chip, drug administration system, wireless power management, and data transmission equipment of the contact lens were integrated into a biocompatible polymer. Due to their high transparency (>91%) and elasticity (25%), hybrid graphene-Ag nanowires were utilized in the proposed contact lens for the sensor and wireless antenna. The contact lens was examined using typical blood glucose measurements and rabbit models. To restore normal glucose levels, the drug reservoirs were electrically energized to release the medication. Using the electronic device's resistance and capacitance, Kim et al. developed a multifunctional contact lens sensor for monitoring intraocular pressure and tear glucose levels.[28] The sensing device was constructed using an array of nine field-effect transistors with a graphene channel and hybrid source-drain electrode. Utilizing π–π stacking with a pyrene linker, glucose oxidase (GO_x) was immobilized on the graphene channel for selective and sensitive glucose detection. Atomic force microscopy verified the precise attachment of GO_x to the graphene channel's surface. The GO_x-based biosensor worked by catalyzing the oxidation of glucose in the presence of oxygen to produce gluconolactone, which was hydrolyzed to yield gluconic acid and hydrogen peroxide (H_2O_2). As glucose concentration increased, the concentration of H_2O_2 increased, and the oxidation of H_2O_2 lead to more charge carriers in the channel and, consequently, a higher drain current. However, various difficulties must be addressed before clinical applicability may be achieved. These EC sensors relied on enzymes, which are intrinsically unstable and rapidly deteriorate, hence restricting their effectiveness over extended time periods. In addition, operational parameters such as ambient oxygen, pH, temperature, and humidity affect sensor performance. In addition, according to health regulations, sterilizing smart contact lenses may denature enzymes.[61] To overcome these limitations of enzymatic sensing, a non-enzymatic contact lens was reported by Lin et al. (Figure 3A-b).[64] The researchers developed a phenylboronic acid (PBA)-based HEMA contact lens to take advantage of the reversible covalent bond

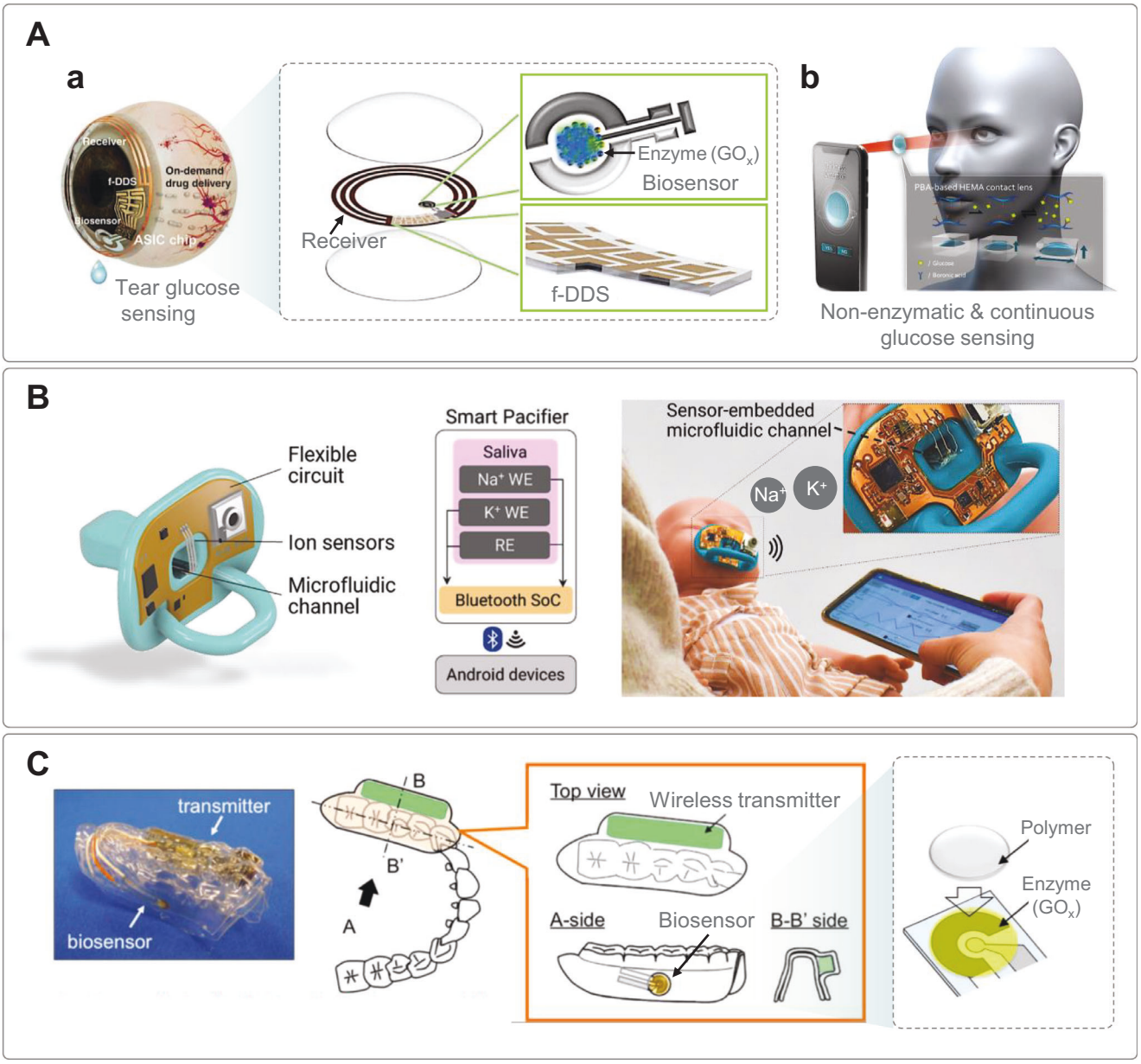

Figure 3. A) Contact lens for glucose monitoring: a) Schematic illustration for diabetic diagnosis and therapy of the smart contact lens embedded with an enzymatic biosensor, a wireless power transmitter, and a remote communication system.[63] b) Smartphone camera system for detecting the thickness of the PBA-based enzyme-free contact lens. Reproduced according to the terms of the CC BY license.[64] Copyright 2018, The authors, published by MDPI. B) Smart pacifier device composed of a flexible circuit and a microfluidic channel embedded with a sensor for continuous monitoring of salivary electrolytes. Reproduced with permission.[12c] Copyright 2022, Elsevier. C) Schematic image of the mouthguard biosensor to custom-fit the patient's dentition. The device consisted of a glucose sensor and wireless transmitter incorporating a potentiostat for stable glucose measurement. Reproduced with permission.[67] Copyright 2016, Elsevier.

between boronic acid and glucose. Absorption of the glucose by the PBA-based contact lens increased hydrophilicity and lead to swelling. Similarly, a low concentration of glucose led to shrinking. By continuously measuring thickness changes of the contact lens using a smartphone camera and image processing, the current level of glucose could be determined. This method has promise for noninvasive glucose monitoring. Like tears, saliva contains several different analytes, which are listed with their corresponding diseases and disorders in Table 1. Research summaries on saliva-based electrochemical sensors are provided in **Table 3**. Saikat et al. have developed a battery-free passive sensor system for wireless salivary pH monitoring.[65] Two components comprise the sensor: A pair of pH electrodes and a transponder system and pH is determined through voltammetry. Communication of the pH data was achieved through a passive transponder system that harvests incoming RF energy to send a digital signal representing the measured pH. Lim et al. created a bioelectronic pacifier for monitoring salivary electrolytes in

Table 3. Summary of EC sensors targeting analytes in saliva.

Target analyte	Detection method	Recognition material	Linear detection range	Limit of detection	Ref.
Glucose	Amperometry	Nb_2O_5-reduced graphene oxide (rGO) composite	1–10 mM	1 mM	[71]
	Amperometry	Enzyme; GO_x	0.1–1.4 mM	—	[66]
	Amperometry	Enzyme; GO_x	1.75 μM–10 mM	—	[68]
pH	Potentiometry	Metal oxide (Sb/Sb_2O_3)	pH 4–9	—	[65]
Na^+	Potentiometry	Sodium ISM (Sodium ionophore X, DOS, PVC, NaTFPB, THF)	10^{-3}–0.1 M	—	[12c]
K^+	Potentiometry	Potassium ISM (KTFPB, Valinomycin, PVC, DOS, THF)	10^{-3}–0.1 M	—	[12c]
Uric acid	Amperometry	Enzyme; uricase	<1 mM	50 μM	[69]

infants (Figure 3B).[12c] The miniaturized technology permits the seamless integration of a lightweight, low-profile device with a commercial pacifier without the need for additional fittings or structural alterations. The ion-selective sensors, flexible circuits, and microfluidic channels of the portable gadget simplify noninvasive electrolyte monitoring. The flexible microfluidic tube allows for the continuous and efficient collection of saliva from the mouth. By modifying the surface properties of the channels and the construction of the capillary reservoir, reliable pumping of the viscous medium for quick calibration and measurement is achieved. The system's embedded sensors exhibit good stability and sensitivity: 52 and 57 mV per decade for the sodium and potassium sensors, respectively. In vivo testing with babies in the critical care unit demonstrates the device's practicability and effectiveness in the saliva-based detection of vital electrolytes without artificial stimulation. García-Carmona et al. developed an enzyme-based electrochemical pacifier for detecting glucose levels in saliva.[66] This baby-friendly device incorporated saliva collecting, electrochemical sensors, and small wireless electronics on a single pacifier platform. The newborn's mouth movements while sucking on the pacifier encouraged efficient saliva pumping and unidirectional flow from the mouth to a chamber outside the oral cavity that contained the enzymatic biosensor. The platform's glucose detection capabilities in both healthy and diabetic individuals were evaluated and linked with their blood glucose levels, which revealed the sensor's exceptional performance. This integration enabled real-time and selective monitoring of the infant's health, constituting the first infant-focused wearable sensor for chemical saliva detection. Arakawa et al. have developed a detachable "Cavitas sensor" for noninvasive saliva glucose monitoring in the mouth cavity (Figure 3C).[67] The Cavitas sensor features a poly(2-methacryloyloxyethyl phosphorylcholine-*co*-(2-ethylhexylmethacrylate) coating for improved GO_x attachment and a cellulose acetate membrane to protect the sensor from mucin contamination and signal interference caused by ascorbic acid and uric acid.[68] Cavitas sensors can therefore consistently measure glucose levels in saliva without the need for pretreatment and the saliva glucose levels can be correlated to blood glucose levels. Similarly, salivary uric acid levels can be measured to provide noninvasive, real-time monitoring of uric acid levels. Wang et al. presented an integrated, wireless, amperometric mouthguard biosensor for the real-time monitoring of salivary uric acid levels.[69] Uricase catalyzes the oxidation of uric acid and the generation of H_2O_2, which is subsequently reduced at a Prussian blue modified electrode. The resulting current enables the detection of uric acid levels in saliva. Due to the complexity of saliva, electropolymerized o-phenylenediamine was created to prevent biofouling and electroactive species from adhering to electrodes. In addition, a Bluetooth-enabled circuit board was inserted into the mouthguard to capture wireless data. Because the close relationship between blood and salivary uric acid has been demonstrated in the past, salivary uric acid levels provide a noninvasive alternative of determining blood uric acid levels.[70]

2.2.7. Electrochemical Sensors Targeting Breath

Breath is generally considered as gas-phased human biofluid, incorporating many gas molecules, exogenous metabolites, and even viral particles.[75] In general, biomarkers for breath analysis include volatile and semi-volatile organic compounds (VOCs and SVOCs), in addition to typical gases like CO_2 and NO as more than 250 different types of VOCs have been found in exhaled breath.[76] For example, isopropyl alcohol and fatty acid derivatives (e.g., pentane) are considered a potential factor indicative of inflammation. Even though the solid relationship between those organic gas molecules and specific diseases needs to be clarified and verified, medical diagnosis and screening methods targeting breath could give several unbeatable advantages over an analysis of other biofluids based on enormous kinds of informative particles in a breath.[77] The diseases which could be linked to the major analytes found in exhaled breath are listed in **Table 4**. Recent research on electrochemical sensors based on the human breath is summarized in **Table 5**.

Exhaled Breath Temperature and Respiration Rate: Some research on intelligent face masks with integrated heat flux sensors has been reported.[15,59b,91] This sensing platform allows for verification of the mask's appropriate fit based on recorded temperatures and breathing rate information. In addition, a coughing event can be diagnosed by detecting sudden temperature fluctuations.

Detection of Glucose and Common Gases: Jeerapan et al. presented a glucose-detectable face mask that enables continuous monitoring with its own self-powered biosensing system. (**Figure 4**A).[92] This biosensor demonstrated that a two-electrode-based biomask enables real-time glucose sensing without further accessories such as a signal amplifier or external energy applied, generating the current within a linear glucose

Table 4. Target analytes and their typical amounts in exhaled breath.

Analyte	Concentration range	Reflecting human health status and diagnostic application	Ref.
Acetone	148–2744 ppb[a)]	Metabolic rate, diabetic ketoacidosis, starvation	[78]
Alcohol	13–1000 ppb for ethanol; 160–2000 ppb for methanol	Blood alcohol concentration (BAC), Alzheimer, breast cancer	[76, 79]
Alkane	1–5 ppb[b)]	Lung cancer, chronic renal failure/ureimia	[80]
Aromatics	50–250 ppm[a)]	Alzheimer, breast cancer, colorectal cancer	[81]
NO	10–50 ppb[b)]	Asthma, liver transplant rejection, chronic pulmonary obstructive disease, and cystic fibrosis	[82]
CO	0–5 ppm[a)]	Smoking status, inflammatory diseases of the lung and other organs	[83]
CO_2	≈40 000 ppm[a)]	Inflammation	[84]
NH_3	248–2935 ppb[b)]	Liver disease or dysfunction, renal failure, cirrhosis of liver, peptic ulcer, halitosis	[85]
Isoprene	22–234 ppb[b)]	Hypoxia/respiratory status	[78]

[a)] Parts per million [b)] Parts per billion.

Table 5. Summary of EC sensors targeting analytes in breath.

Target analyte	Detection method	Recognition material	Linear detection range	Limit of detection	Ref.
Rate of respiration (indirectly measuring H_2O)	Conductometry (2-electrode)	Carbon	—	—	[86]
H_2O	Capacitive	Fibrous Ag/polyimide	6–97% R.H.	—	[87]
NH_3	Impedimetric	Inkjet-printed polyaniline (PANI) nanoparticles	40–2993 ppbv[a)]	—	[85]
Isoprene	Resistive	Selective isoprene detection of Ti^{4+}	5–500 ppb[b)]	5 ppb	[88]
Nitrite	Square wave voltammetry (SWV)	Reduced graphene oxide (rGO)-integrated electrode	20–100 μM	830 nM	[89]
Limonene[c)]	Differential pulse voltammetry (DPV)	Hexanethiol modified Au nanoparticles	0.005–0.05 mM	0.2 mmol L^{-1}	[90]

[a)] Parts per billion by volume [b)] Parts per billion [c)] One of VOCs that has been found in the breath of individuals with liver cirrhosis.

concentration range of 0.25–2.50 mM (reported sensitivity: 2.1 μA cm^{-2} mM^{-1}). It can be achieved by a redox reaction: an oxygen reduction in the cathode under the assistance of platinum-poly(3,4-ethylenedioxythiophene) materials, and a glucose oxidation in the GO_x- and tetrathiafulvalene-functionalized bioanode. Yet, the glucose concentration in the breath, compared to other biofluids such as a tear, saliva, and sweat, showed a drastically low level, and therefore less considered as a biomarker in the breath. Furthermore, since breath consists mostly of water vapor, it might significantly decrease sensing performance as the vapor molecules condense toward active sensor electrodes and hinder the effective electrochemical reaction. Therefore, utilizing additional accessories such as a condenser, cold trap, or desiccant could be considered as a potential way for continuous monitoring of target analytes with improved sensitivity.[93] It has been reported that sensing the acetone within the breath cross-interacted with the water vapor. It leveraged a dehumidifying system to successfully detect significantly low acetone concentration in dry breath samples within the detection limit of 1.6 ppm.[94]

Hibbard et al. developed a system for measuring NH_3 in human breath based on a single-use, disposable, inkjet-printed impedimetric NH_3 sensor made from polyaniline nanoparticles (Figure 4B).[85] The device was designed for NH_3 sampling in human breath samples by addressing some challenges such as variations in breath sample volume, flow rate, oral NH_3 sources, temperature, and humidity. It was proven that NH_3 in the breath of patients with end-stage renal disease reduced dramatically after dialysis and associated well with blood urea nitrogen, indicating that low-cost point-of-care breath NH_3 devices might be used as a noninvasive tool for monitoring and treating kidney failure.

Humidity Sensor: Güder et al. designed a paper-based humidity sensor that can be attached to a mask to monitor respiration in real-time.[86] The sensing system was developed by digitally printing graphite ink onto cellulose paper, connecting it to the signal processing unit, and integrating it with a mask. Generally, exhaled breath is fully humidified (relative humidity of 100%), which increases the number of water molecules on the sensor and subsequently its ionic conductivity. Inhaling lowers the amount of moisture on the surface of cellulose fibers because the relative humidity of the surrounding environment is often lower than that of exhaled air. This sensing system uses a two-electrode amperometry to electrolyze the absorbed moisture and

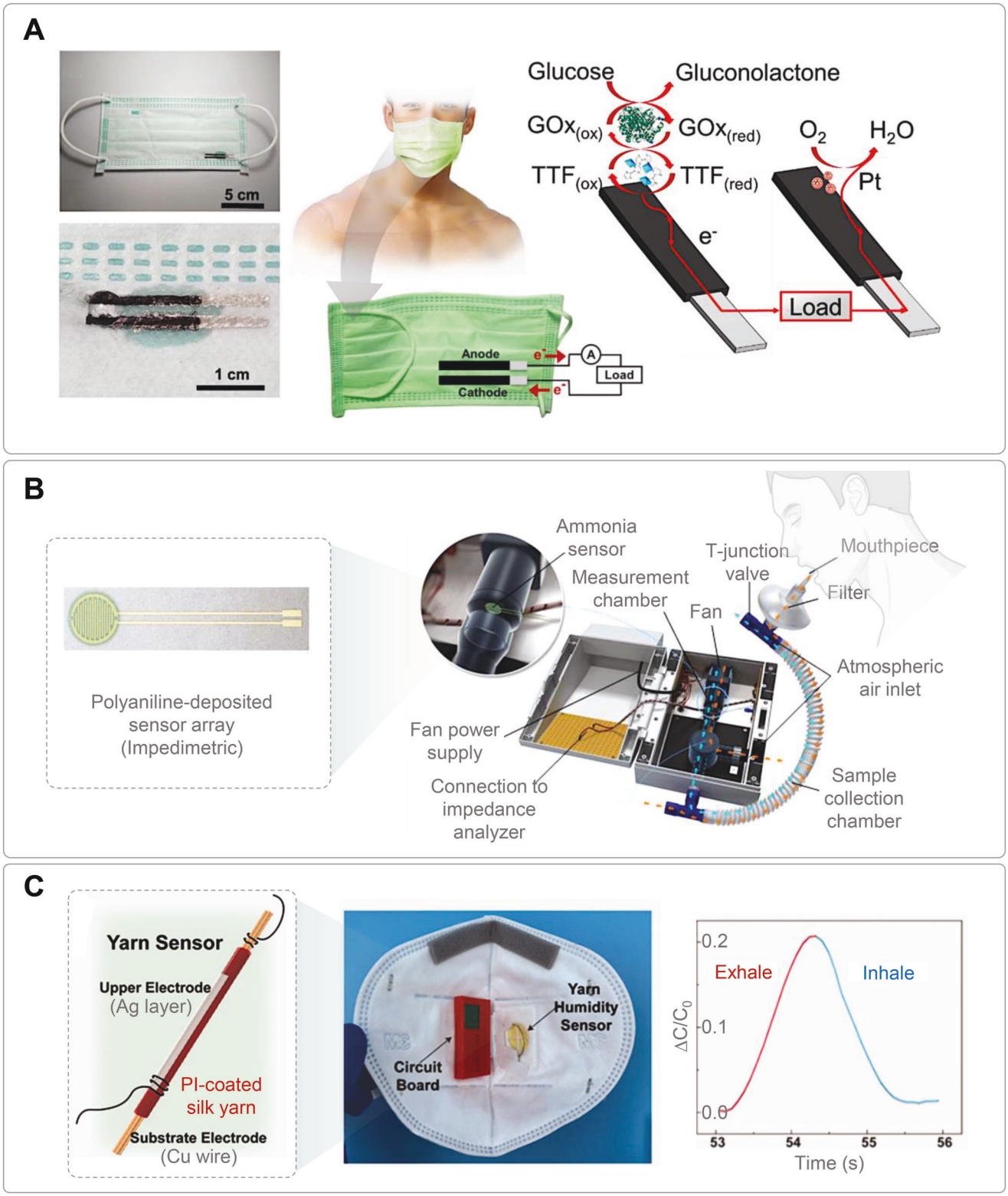

Figure 4. A) Self-powered-biosensor-integrated smart facemask for wireless glucose monitoring. Reproduced according to the terms of the CC BY license.[92] Copyright 2022, The authors, published by Elsevier. B) Breath ammonia measurement system consisting of the printed ammonia sensor and the breath monitoring device. Reproduced with permission.[85] Copyright 2013, American Chemical Society. C) Smart mask with embedded capacitive humidity sensor and a measured signal of a one-respiratory cycle. Reproduced with permission.[87] Copyright 2021, SAGE Publications.

Table 6. Target analytes and their concentration ranges in urine.

Analyte	Concentration range	Reflecting human health status and diagnostic application	Ref.
Na^+	65–175 mM	Cystic fibrosis, muscle cramp, hyper/hyponatremia	[98]
K^+	15–70 mM	Hyper/hypokalemia and an indicator of ocular disease	[98]
Cl^-	50–170 mM	Cystic fibrosis, lung disease, Hyper/hypochloremia, and potentially for hydration status and electrolyte stores	[98]
Lactic acid	<1.1 mM	Lower urinary tract infection (cystitis), upper urinary tract infection (pyelonephritis), urinary tract obstruction	[99]
Urea	9.3–23.3 g L^{-1}	Renal function, metabolism status	[100]
Glucose	<0.25 mg mL^{-1}	Glycosuria	[101]
Benzaldehyde	5–50 ppm	Early disease/metabolism diagnosis	[102]
Piperitone	25–200 ppm	Diagnostics of bladder cancer	[103]

measure the amount of current produced from subsequent redox reactions. Using this tool, they can accurately assess the pace and rhythm of a person's breathing. The gadget does not require calibration since the sensor measures moisture content variations between inhaled and exhaled air. Similarly, Ma et al. suggested a capacitive humidity sensor that combines signal collection with a wireless communication system for monitoring human breath (Figure 4C).[87] Due to its high water-permeability, chemical stability, and thermal stability, polyimide (PI) was selected as the humidity-sensitive material and dielectric layer material in the capacitive humidity sensor. Owing to a negative charge of the PI layer, it can precisely detect the proportionate absorption of water molecules, which corresponds to an increase in the environmental humidity. Typically, the dielectric constant of PI falls between 2.9 and 3.7, but the dielectric constant of molecular water is substantially higher (≈78.54). As a result, a higher humidity leads to a rise in the dielectric constant and a change in capacitance.

2.2.8. Electrochemical Sensors Targeting Urine

The main target analytes in urine and their associated health conditions, and an overview of the state-of-the-art related studies on the urine-based electrochemical sensors is shown in **Tables 6** and **7**, respectively. Zhang et al. developed a diaper-integrated, self-powered enzymatic biosensor for measuring urine glucose

Table 7. Summary of EC sensors targeting analytes in urine.

Target analyte	Detection method	Recognition material	Linear detection range	Limit of detection	Ref.
Glucose	Amperometry	Enzyme; GO_x	1–5 mM	—	[95]
	Amperometry	Enzyme; GO_x	1–16 mM	—	[96]
	Amperometry	Enzyme; GO_x	0–14 mM	15.5 μM	[97]
Lactate	Amperometry	HS-NiS/NiF[a)]	0.5–88.5 μM	0.023 μM	[104]
	Amperometry	NiS-NC@NiS-MS/NiF[b)]	0.5–88.5 μM	0.5 μM	[105]
Uric acid	Amperometry	Enzyme; UO_x	0.1–0.6 mM	—	[96]
	Amperometry	Enzyme; UO_x	0–4 mM	15.3 μM	[97]
H_2O_2 (reactive oxygen species)	Amperometry	Catalyst: Pt/CNT/Au	0–2.5 mM	111.5 μM	[97]
Acetoacetate acid	Amperometry	Enzyme; D-β-hydroxybutyrate dehydrogenase (HBDH) and nicotinamide adenine dinucleotide (NADH)	6.25–100 mg dL^{-1}	6.25 mg dL^{-1}	[106]
Valine	Square wave voltammetry	Modified carbon paste electrode (CPE) with electropolymerized Ag nanoparticles capped with saffron (AgNPs@Sa)	0.258–11.94 ng L^{-1}	0.097 ng L^{-1}	[107]
Na^+	Potentiometry	ISEs (modified with the corresponding selective ionic membrane)	10–160 mM	1 mM	[97]
K^+	Potentiometry	ISEs (modified with the corresponding selective ionic membrane)	2–32 mM	1 mM	[97]
Digoxin	Differential pulse voltammetry (DPV)	ZnCo-based metal-organic frameworks (MOFs)	1–5 nM	5.89 pM[c)]	[108]
Dopamine	Differential pulse voltammograms	Au nanoparticles/β-Cyclodextrin/Nafion-modified Au electrode	0.05–20 μM	0.6 nM	[109]

[a)] Hollow sphere structured nickel sulfide [b)] Nanoclusters of nickel-sulfides (NiS) on NiS microsphere on a bare nickel foam substrate [c)] For the sake of convenient comparison, value previously reported in ng mL^{-1} was converted to pM, based on a molecular weight of digoxin (i.e., 780.938 g mol^{-1}).

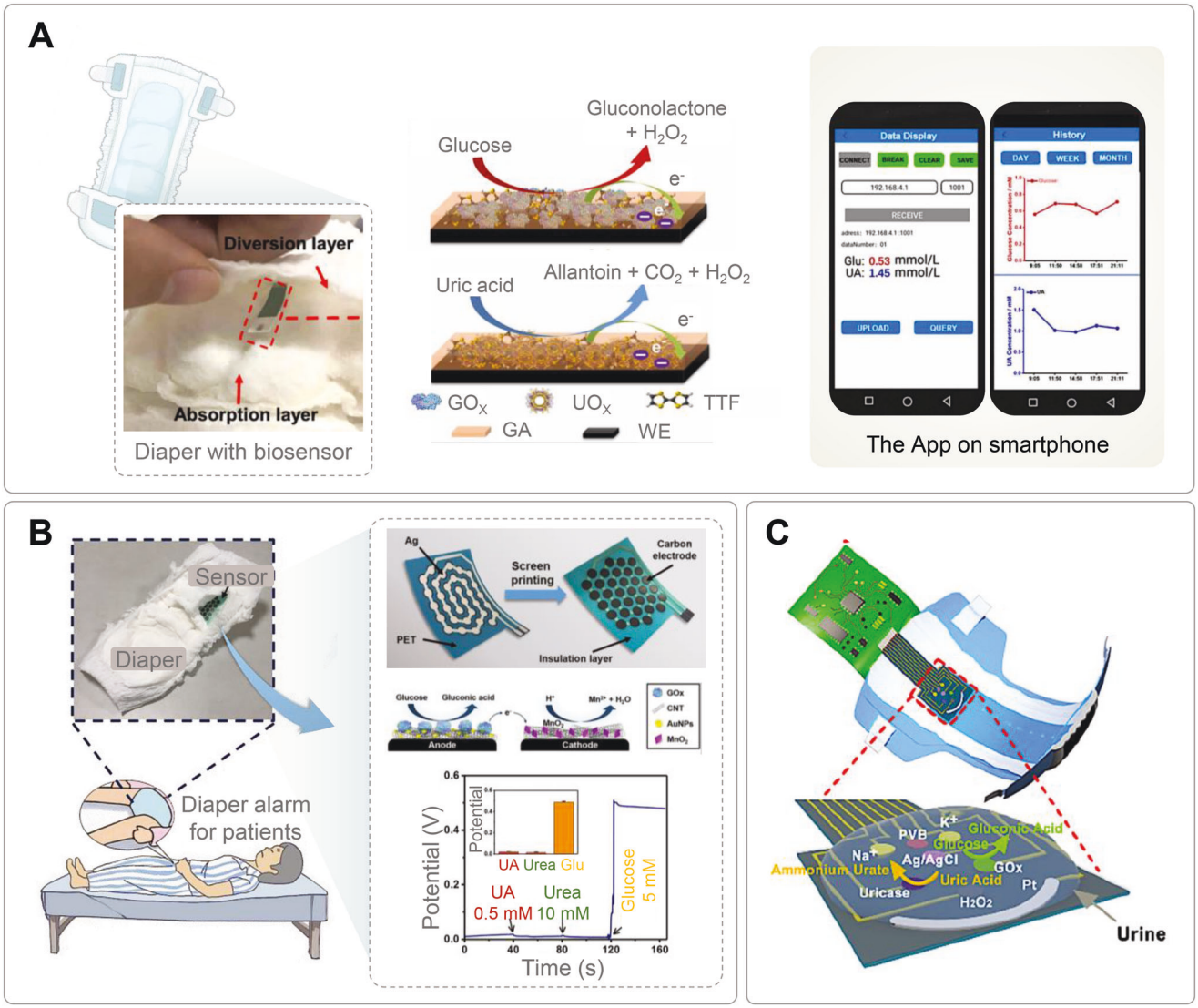

Figure 5. A) Glucose- and uric acid-detectable diaper with biosensor and customized smartphone application. Reproduced with permission.[96] Copyright 2022, Elsevier. B) Diaper alarm device with embedded carbon-based enzymatic biofuel cell. Reproduced with permission.[95] Copyright 2021, Elsevier. C) Smart diaper which enabled simultaneous and selective monitoring of urinary metabolites (e.g., reactive oxygen species, glucose, and uric acid) and electrolytes (e.g., Na^+, K^+). Reproduced with permission.[97] Copyright 2022, American Chemical Society.

levels in diabetic patients (**Figure 5**A).[95] The gadget was powered by an enzyme biofuel cell (EBFC) that produced energy from the glucose present in urine. When a diaper containing EBFC was worn, the LED flashing rate indicated the glucose concentration in the urine. The biosensor system composed of EBFC, PMS, and LED was a self-powered sensor system that measured the glucose level in the urine of diabetic patients without the need for additional power. To investigate the impact of potential interfering chemicals on glucose detection, the sensor's selectivity and anti-interference capacity were evaluated by adding uric acid and urea as potential interfering substances. There was minor disruption with repeated administration of uric acid and urea, but the well-defined signal response could still be obtained with 5 mM glucose. This study indicated that the presence of interfering species had no influence on the practical measurement of glucose. They also noticed that pH had no influence on the biosensor's performance owing to glucose oxidase's tolerance (GO_x). Both outstanding anti-interference capability and selectivity were exhibited as they showed high-performance detection of urine glucose using the produced biosensor. Using the same procedure, they prepared eight biosensors to validate their reproducibility. The coefficient of variation for the results of eight measurements was calculated to be 3.7%, exhibiting the small fluctuation in output from each sensor and indicating that the biosensor can be replicated. Su et al. proposed the diaper-mounted wearable smart sensor for in situ urine biomarker detection. (Figure 5B).[96] Due to the difficulties of collecting urine from patients with urinary incontinence, the researchers developed a low-cost and practical device to detect urine in situ for these patients. A diaper fitted with an electrochemical biosensor, a portable detection device, and a

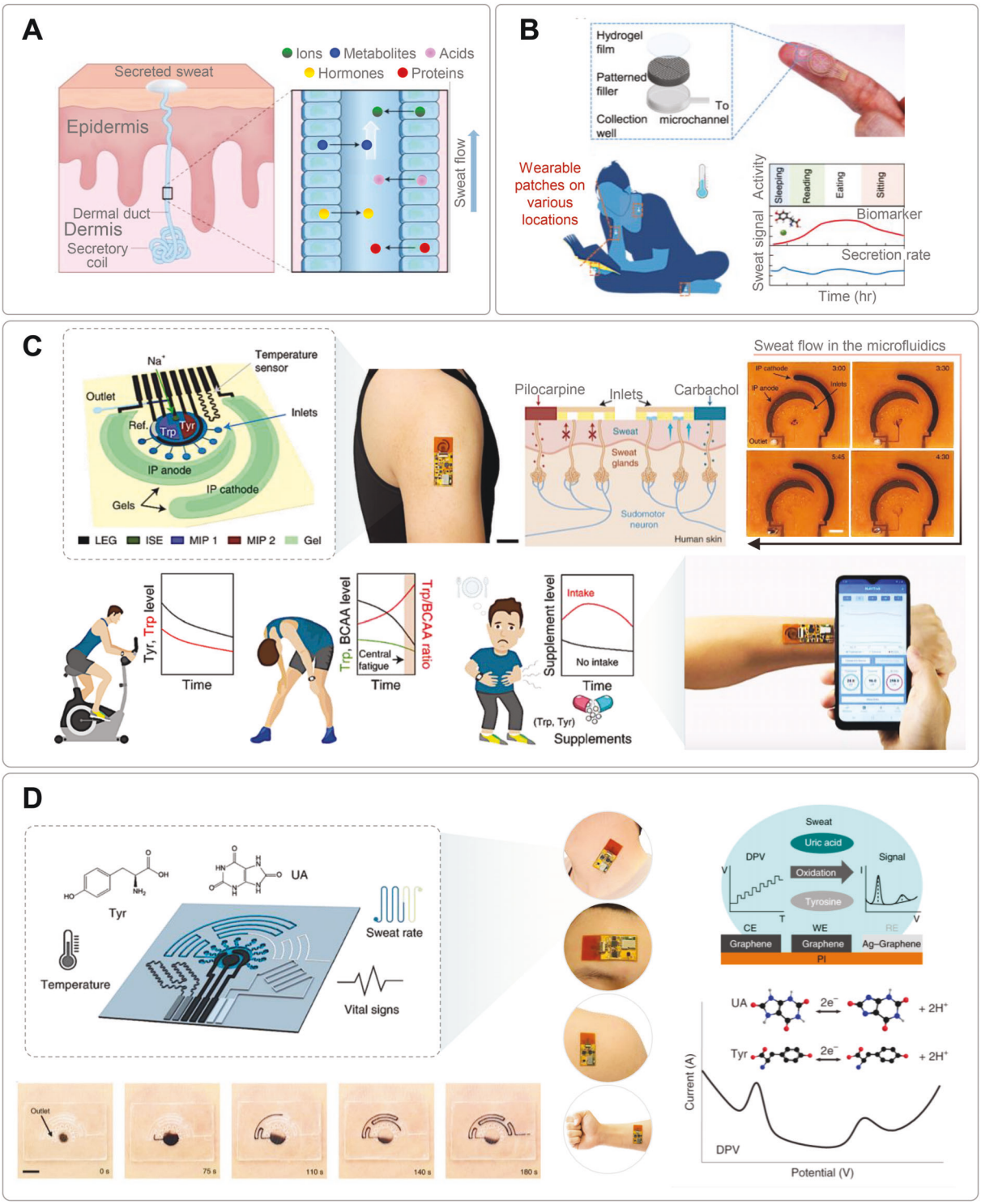

Figure 6. A) Sweat gland structure and biomarker partitioning. Eccrine sweat glands are comprised of a secretory coil where sweat is first generated and a dermal duct that conveys sweat through the epidermis to the skin surface. In the process, a variety of analytes including ions, metabolites, acids, hormones, and proteins and peptides are partitioned into sweat from nearby blood and interstitial fluid. Reproduced with permission.[110] Copyright 2018, Springer Nature. B) Wearable patches for continuous sweat monitoring (integrating electrochemical sensors for pH, Cl^-, and levodopa monitoring) at rest. Reproduced according to the terms of the CC BY license.[112] Copyright 2021, The authors, published by Springer Nature. C) Schematic of the wearable sweat sensor (i.e., NutriTrek) that enables metabolic monitoring such as a continuous on-body tryptophan (Trp), tyrosine (Tyr), branched-chain amino acid (BCAA), and sweat amino acid (AA) level analysis in different conditions. Reproduced with permission.[12b] Copyright 2022, Springer Nature. D) Real-time, continuous in situ measurement of respiration rate, temperature, sweat uric acid, and tyrosine levels. Reproduced with permission.[51] Copyright 2022, Springer Nature.

Table 8. Target analytes and their typical amounts in sweat.

Analyte	Concentration range	Reflecting human health status and diagnostic application	Ref.
Na^+	66.3 ± 46.0 mM	Cystic fibrosis, muscle cramp, hyper/hyponatremia	[113]
K^+	9.0 ± 4.8 mM	Hyper/hypokalemia and an indicator of ocular disease	[114]
Cl^-	10–100 mM	Cystic fibrosis, lung disease, hyper/hypochloremia, and potentially for hydration status and electrolyte stores	[114]
Glucose	100–200 μM	Diabetes management, metabolic syndrome	[115]
Lactate	5–20 μM	Fatigue level, lactic acidosis, ischemia, sepsis, liver disease and cancer, hydration plan	[18e]
Uric acid	2–10 mM	Gout, arthritis, heart disease diabetes, cardiovascular diseases	[116]
Ethanol	2.5–22.5 mM	Metabolic rate	[117]
Urea	22.2 ± 8.0 mM	Renal function, metabolism status	[18e]
Cortisol	8.16–141.7 ng mL^{-1}	Psychological stress (anxiety), stress disorder, Cushing syndrome, Addison's disease	[118]
Skin temperature	25–36 °C[a)]	Thermal stress	[66]
Tyrosine	66–300 μM	Metabolic disorders, gout	[49, 119]
Tryptophan	20–91 μM	Anxiety, nerve damage	[120]

[eqa)] On peripheral spot-on skin.

smartphone application for data processing were fully integrated into the system. A urine-resistant enzymatic biosensor with a self-locking valve was put between the diversion and absorption layers of a standard diaper to measure the urine during urination. GO_x and uric acid oxidase (UO_x) were immobilized on the biosensor to detect glucose and uric acid from the urine, respectively. These enzymes react with glucose or uric acid, producing an electron transfer between the enzyme and electrode, where the electrode collected electrons to provide an analog electrical current signal proportional to glucose or uric acid concentrations in urine. A smartphone application was used to collect the wireless sensor data and display a plot of the urine biomarkers over time. This biosensor detected urine with good sensitivity, linearity, and selectivity, and it was compatible with portable detection equipment. The relative longevity of each biosensor was also evaluated. Even after 20 days, fewer than 10% of the biosensors' response activity had diminished. The reported wearable sensing system not only provided doctors with real-time measurement data of urine biomarkers to assess the patient's health status, but also reminded nurses to change a patient's diaper on time, demonstrating great application potential for caring for disabled elderly in nursing homes. Li et al. proposed an integrated array of multiplex electrodes for urine monitoring (Figure 5C).[97] They proposed a mechanically flexible and intelligent diaper for in situ urinalyses that concurrently and selectively monitored urine metabolites, such as glucose, reactive oxygen species, and uric acid, and electrolytes (e.g., Na^+, K^+). The arrays of sensor electrodes were modified with carbon nanotube coatings, ion-selective membranes, enzymes, and Pt nanoparticles to provide highly selective and sensitive monitoring of urine-related target biomarkers. ISEs displayed good linearity, with average sensitivities of 63.08 mV per decade for Na^+ and 61.01 mV per decade for K^+, respectively. The CNT-loaded, flexible electrode modified with various active substances (enzyme or Pt particles) demonstrated a broad linear response range and outstanding sensitivity for the detection of test chemicals (H_2O_2, 26.9 A mM^{-1}; uric acid, 0.53 A mM^{-1}; glucose, 2.71 A mM^{-1}). Each sensor had a detection limit of 111.5 μM for H_2O_2, 15.3 μM for uric acid, 15.5 μM for glucose, 1 mM for Na^+, and 1 mM for K^+.

2.2.9. Electrochemical Sensors Targeting Sweat

Sweat is a suitable biofluid for non-invasive biosensing of analytes since it possesses many detectible analytes that provide a full understanding of a person's health. As electrolytes, metabolites, acids, hormones, proteins, and peptides actively and passively diffuse from the surrounding blood and interstitial fluid into a sweat, it is possible to identify them on the skin (**Figure 6**A).[110] Continuous monitoring of the analytes is essential for maintaining optimal physiological homeostasis.[60b] The sensing system for non-invasive sweat monitoring is flexible and wearable, setting it apart from other biofluid sensors. Because sweat sensing systems must stay attached to the skin throughout a variety of body activities, the resilience of the sensors to mechanical strain should be a key element in evaluating sensors.[111] There are two primary kinds of non-invasive EC sensors for monitoring perspiration—fabric/flexible plastic-based devices and sensors printed directly on the epidermis (temporary tattoo).[60b] **Table 8** shows the main analytes that can be found in sweat and their associated diseases. **Table 9** gives an overview of the most recent studies on sweat-based electrochemical sensors.

pH and Electrolytes: Nyein et al. reported a patch for continuous analysis of thermoregulatory perspiration during rest (Figure 6B).[112] They utilized hydrophilic fillers for rapid perspiration absorption into the sensor channel, hence drastically decreasing the necessary sweat accumulation time for real-time monitoring. In addition to sweat rate sensors, EC sensors for monitoring pH, Cl^-, and levodopa were also integrated. Multiplexed sensing of all three analytes is also advantageous since enzymatic sensors, such as the levodopa sensor, can be affected by sample pH and ionic strength; consequently, simultaneous monitoring of these influencing parameters can be crucial for converting sensor signals into meaningful concentration readings. Each pH and

Table 9. Summary of EC sensors targeting analytes in sweat.

Target analyte	Detection method	Recognition material	Linear detection range	Limit of detection	Ref.
Glucose	Amperometry	PET-based Au electrodes	0.02–1.11 mM	2.7 μM	[121]
	Amperometry	Carbon graphite ink on adhesive tapes	0.48–2.59 mM	0.80 μM	[122]
	Amperometry	SBPthi nanosheets[a)]	0.82 μM–4.0 mM	0.27 μM	[123]
	Amperometry	Au-Pt nanoparticles	0.01–10 mM	3 μM	[124]
	Amperometry	Pt/Au nano-alloy	1.39–13.9 mM	482 μM	[125]
	Amperometry	Enzyme: GO_x	0–0.9 mM	10 μM	[126]
	Amperometry	Enzyme: GO_x	≈2.1 mM (Dynamic)	300 nM	[127]
Lactate	Potentiometry	Prussian blue/LO_x	0–1.0 mM	—	[51]
	Amperometry	Enzyme: LO_x	10 pM–20 mM	≈1.26 nM	[128]
	Impedimetric	PANI/PBA-pNIPAM @CNC/CNT[b)]	1–25 mM	0.10 ± 0.04 mM	[129]
	Electrochemical impedance spectroscopy	LO_x-GO nanosheet	1.3–113.4 mM	1 mM	[130]
Uric acid	Cyclic voltammetry	Laser-engraved graphene (LEG)	10–50 μM	0.74 μM (Minimum)	[49]
Electrolyte (NaCl)	Impedimetric	PANI/PBA-pNIPAM @CNC/CNT[a)]	3–80 mM	0.23 mM	[129]
Na^+	Potentiometric	Carbon black nanomaterials	10^{-4}–1 M	63 μM	[131]
K^+	Potentiometric	PEDOT/POT	3.31–7.25 mM	—	[132]
Cl^-	Electrochemical impedance spectroscopy	Gold microelectrodes	10–100 mM	100 mM	[133]
pH	Potentiometry	pH-sensitive electrode (graphite-polyurethane composite)	pH 5–9	—	[42]
	Potentiometry	pH-sensitive electrode (graphite-polyurethane)	pH 6–9	—	[134]
Alcohol	Amperometry	Enzyme: AO_x	0.01–13.0 mM	—	[135]
	Amperometry	Enzyme: AO_x	3.0–36.0 mM	—	[117]
Ethanol	Amperometry	Carbon, Ag	≈1 mM L^{-1}	—	[136]
Urea	Cyclic voltammetry	NiCu (OOH)	2.00–30.00 mM	—	[137]
Cortisol	Cyclic voltammetry /differential pulse voltammetry	ZnO nanorods, anti-cortisol antibody	1 fg mL^{-1}–1 μg mL^{-1}	0.45 fg mL^{-1} (CV) 0.098 fg mL^{-1} (DPV)	[138]
Tyrosine	Cyclic voltammetry	Laser-engraved graphene (LEG)	25–140 μM	3.6 μM	[49]
Tryptophan	Cyclic voltammetry	Laser-engraved graphene (LEG)—Molecularly imprinted polymer (MIP)	0–400 μM	—	[12b]
Trace metal (Zn)	Square wave anodic stripping voltammetry (SWASV)	Bismuth/Nafion	0.1–2.0 μg mL^{-1}	1 μg mL^{-1}	[111]

[a)] Poly(aniline/phenylboronic acid)—Poly(*N*-isopropylacrylamide) @ conductive nanoporous carbon nanotube-cellulose nanocrystals. [b)] SBP_{Thi}: a flexible electroactive Schiff base polymer

Cl^- sensor was manufactured with PANI and commercially available silver ink, respectively. This sensor demonstrated excellent pH (range: pH 4 to 8) and Cl^- performance (range: 25–200 mM).

Metabolites: Flexible sweat sensors with gold nanopine needles (AuNNs) were developed by Yu et al. for sensitive real-time monitoring of glucose and lactate concentrations in human perspiration.[6c] Following the manufacturing of the sensor chips, AuNNs were fabricated on flexible gold substrates by electrochemical deposition for signal amplification. The corresponding enzymes were cross-linked to the chip, followed by monitoring the glucose and lactate concentrations in human sweat in real-time. Poletti et al. also established continuous monitoring of glucose and lactate in human sweat using the enzymatic sensors and capillary flow.[139] Enzymes (i.e., GO_x and LO_x) were attached to a graphene oxide and chitosan composite to achieve durable and stable deposition on the electrochemical platform. The

sensing signal remained steady and linear for 2 h in a concentration range of glucose and lactate between the limit of quantification (32 and 68 nM, respectively) and the upper limit of linearity (3.8 and 50.0 mM, respectively). The device is straightforward, sturdy, and dependable, and it can be worn without direct contact of the active part with the skin, making it suitable for concurrently monitoring of glucose and lactate in human sweat.

Sweat Alcohol: Kim et al. demonstrated a tattoo-based iontophoretic biosensing system for non-invasive sweat alcohol monitoring.[117] This wearable prototype allowed for the transdermal injection of pilocarpine to induce perspiration through iontophoresis and the amperometric detection of ethanol in sweat utilizing the alcohol-oxidase enzyme and the Prussian blue electrode transducer. The novel biosensor with skin compatibility exhibited a very selective and sensitive reaction to ethanol.[7]

Multivariate Sensing: Due to the lack of a suitable continuous monitoring strategy beyond ion-selective and enzymatic electrodes or direct oxidation of electroactive molecules, the currently reported wearable electrochemical sensors have primarily focused on a limited number of analytes, including electrolytes, glucose, and lactate. With continuing invention and improvement, however, the multivariate detecting capabilities of sweat sensors have advanced significantly.

By carefully combining mass-producible laser-engraved/laser-induced graphene (LEG or LIG), electrochemically synthesized redox-active nanoreporters, molecularly imprinted polymer (MIP)-based "artificial antibodies," as well as novel in situ regeneration and calibration technologies, Wang et al. demonstrated a universal wearable biosensing strategy (Figure 6C).[12b] Two carbachol-loaded iontophoresis electrodes, a multi-inlet microfluidic module, a multiplexed MIP nutrition sensor array, a temperature sensor, and an electrolyte sensor make up the disposable sensor patch. With the help of this technique, it is possible to show the sensitive, selective, and continuous monitoring of a wide range of trace-level biomarkers in biofluids, such as the nine essential amino acids, vitamins, metabolites, and lipids that are typically found in human sweat. The wearable sweat sensing technology "NutriTrek" is the result of the seamless integration of this novel approach with in situ signal processing and wireless communication and can perform individualized and non-invasive metabolic and nutritional monitoring for the purpose of prompt intervention. Combining carbachol iontophoresis-based sweat induction with efficient microfluidic-based sweat collection allows for extended autonomous and continuous molecular analysis with outstanding temporal resolution and accuracy spanning activities, physical exertion, and rest. By enrolling healthy subjects and patients for individualized monitoring of central fatigue, standard dietary intakes, nutrition status, metabolic syndrome risks, and COVID-19 severity, they validated the system in multiple human trials using these five essential or conditionally essential amino acids as exemplar nutrients.

Yang et al. reported a completely laser-engraved sensor for simultaneous sweat collection, chemical detection, and monitoring of vital signs (Figure 6D).[49] As a result of the graphene-based chemical sensor's fast electron mobility, high current density, and ultra-large surface area, their laser-engraved multimodal sensor enabled efficient microfluidic sweat sampling, rapid, and accurate detection of uric acid and tyrosine in human sweat in situ and multiplexed vital-sign sensing. In addition, they underlined that its manufacture was likely to be scalable since all three key modules (physical sensors, chemical sensors, and microfluidic module) were made utilizing LEG from a commonly available CO_2 laser engraving technology.

3. Conclusion and Outlook

This review discusses various electrochemical sensors and their applications for detecting analytes in biofluids. By monitoring the body's physiological condition, we are now several steps closer to meeting the need for proactive health care, thanks to the continued research and development of wearables. However, despite the tremendous attention of several participants in this subject, more work still needs to be done. For instance, the relationship between the concentration of the target analytes in biofluids and their time delay due to diffusion must be established. Also, it is vital to building the sensor to produce a normalized and accurate response, which may require internal calibration. Furthermore, the sensitivity and longevity of this kind of sensor, particularly the enzymatic sensor, should be further improved. Even though the limit of detection of traditional enzyme-based biosensors is typically between 1–100 μM, many critical analytes have low concentrations (1 μM). Due to the low stability of enzymes, there should be an increased focus on developing chemical sensors with superior interference rejection. In addition, other biorecognition components or assay methods (e.g., aptamers) might be used to enhance sensitivity and simplify prolonged usage. Finally, the creation of customized sensors and associated monitoring conditions, storage, and stability should be considered. If critical hurdles are addressed, we envision the wearable electrochemical sensors will provide new possibilities for continually monitoring the human body across various biomedical and fitness applications.

Acknowledgements

J.L., M.C.K., and I.S. contributed equally to this work. The authors acknowledge the support from the IEN Center for Human-Centric Interfaces and Engineering at Georgia Tech and the NSF Engineering Research Center for Cell Manufacturing Technologies (CMaT; EEC 1648035).

Conflict of Interest

The authors declare no conflict of interest.

Keywords

analytes, biofluids, diagnosis, electrochemical sensors, healthcare

Received: December 3, 2022
Revised: February 4, 2023
Published online: March 6, 2023

[1] a) M. Singer, E. Mendenhall, in *A Companion to Medical Anthropology*, (Eds: M. Singer, P. I. Erickson, C. E. Abadía-Barrero), John Wiley & Sons Ltd., New Jersey, United States, **2022**, Ch. 7. https://doi.org/10.1002/9781119718963.ch7; b) L. Zheng, Y. Liu, C. Zhang, *Sens. Actuators, B* **2021**, *343*, 130131; c) M. Little, C. F. C. Jordens, K. Paul,

K. Montgomery, B. Philipson, *J. Bioethical Inq.* **2022**, *19*, 37; d) A. D. A. P. P. Committee, *Diabetes Care* **2021**, *45*, S175; e) R. Suppiah, J. C. Robson, P. C. Grayson, C. Ponte, A. Craven, S. Khalid, A. Judge, A. Hutchings, P. A. Merkel, R. A. Luqmani, R. A. Watts, f. t. D. S. Group, *Arthritis Rheumatol.* **2022**, *74*, 400; f) A. D. Association, *Diabetes Care* **2021**, *45*, S1; g) L. Shi, D. A. Singh, *Essentials of the U.S. Health Care System*, Jones & Bartlett Learning, Massachusetts **2022**; h) S. S. Jdiaa, R. Mansour, A. El Alayli, A. Gautam, P. Thomas, R. A. Mustafa, *J. Nephrol.* **2022**, *35*, 69; i) R. J. Yong, P. M. Mullins, N. Bhattacharyya, *PAIN* **2022**, *163*, e328; j) K. B. Rubinow, D. R. Rubinow, *Dialogues Clin. Neurosci.* **2017**, *19*, 19; k) A. Vijay, A. M. Valdes, *Eur. J. Clin. Nutr.* **2022**, *76*, 489.

[2] a) B. Mete, E. Vanli, M. Yemisen, I. I. Balkan, H. Dagtekin, R. Ozaras, N. Saltoglu, A. Mert, R. Ozturk, F. Tabak, *Int. J. Med. Sci.* **2012**, *9*, 682; b) C. Barsanti, F. Lenzarini, C. Kusmic, *World J. Diabetes* **2015**, *6*, 792; c) M. Al-Mashat, Doctoral Thesis, Lund University, Faculty of Medicine **2021**. https://portal.research.lu.se/en/publications/assessment-of-pulmonary-blood-flow-in-heart-failure-using-novel-a; d) H. Kasban, M. El-Bendary, D. Salama, *Int. J. Inf. Sci. Intell. Syst.* **2015**, *4*, 37.

[3] M. Zhao, P. S. Leung, *Future Medicinal Chemistry*, **2020**, *12*, 645.

[4] J. Heikenfeld, A. Jajack, B. Feldman, S. W. Granger, S. Gaitonde, G. Begtrup, B. A. Katchman, *Nat. Biotechnol.* **2019**, *37*, 407.

[5] S. Menon, M. R. Mathew, S. Sam, K. Keerthi, K. G. Kumar, *J. Electroanal. Chem.* **2020**, *878*, 114596.

[6] a) Q. Cao, B. Liang, C. Yu, L. Fang, T. Tu, J. Wei, X. Ye, *J. Electroanal. Chem.* **2020**, *873*, 114358; b) A. C. Sun, D. A. Hall, *Electroanalysis* **2019**, *31*, 2; c) M. Yu, Y.-T. Li, Y. Hu, L. Tang, F. Yang, W.-L. Lv, Z.-Y. Zhang, G.-J. Zhang, *J. Electroanal. Chem.* **2021**, *882*, 115029.

[7] A. Salim, S. Lim, *Biosens. Bioelectron.* **2019**, *141*, 111422.

[8] M. Mardonova, Y. Choi, *Energies* **2018**, *11*, 547.

[9] M. Mathew, S. Radhakrishnan, A. Vaidyanathan, B. Chakraborty, C. S. Rout, *Anal. Bioanal. Chem.* **2021**, *413*, 727.

[10] A. G.-M. Ferrari, S. J. Rowley-Neale, C. E. Banks, *Talanta Open* **2021**, *3*, 100032.

[11] D. Sim, M. C. Brothers, J. M. Slocik, A. E. Islam, B. Maruyama, C. C. Grigsby, R. R. Naik, S. S. Kim, *Adv. Sci.* **2022**, *9*, 2104426.

[12] a) N. P. Shetti, D. S. Nayak, K. R. Reddy, T. M. Aminabhvi, in *Graphene-Based Electrochemical Sensors for Biomolecules*, (Eds: P. Worsfold, C. Poole, A. Townshend, M. Miró), Elsevier, Amsterdam, The Netherlands, **2019**, Ch. 10. https://doi.org/10.1016/B978-0-12-815394-9.00010-8; b) M. Wang, Y. Yang, J. Min, Y. Song, J. Tu, D. Mukasa, C. Ye, C. Xu, N. Heflin, J. S. McCune, T. K. Hsiai, Z. Li, W. Gao, *Nat. Biomed. Eng.* **2022**, *6*, 1225; c) H.-R. Lim, S. M. Lee, S. Park, C. Choi, H. Kim, J. Kim, M. Mahmood, Y. Lee, J.-H. Kim, W.-H. Yeo, *Biosens. Bioelectron.* **2022**, *210*, 114329; d) J. Suo, Y. Liu, C. Wu, M. Chen, Q. Huang, Y. Liu, K. Yao, Y. Chen, Q. Pan, X. Chang, H.-y. Chan, G. Zhang, Z. Yang, W. Daoud, X. Li, R. Vellaisamy, X. Yu, J. Wang, W. J. Li, *Adv. Sci.* **2022**, *9*, 2203565; e) K. Kim, H. J. Kim, H. Zhang, W. Park, D. Meyer, M. K. Kim, B. Kim, H. Park, B. Xu, P. Kollbaum, B. W. Boudouris, C. H. Lee, *Nat. Commun.* **2021**, *12*, 1544; f) M. S. Mannoor, H. Tao, J. D. Clayton, A. Sengupta, D. L. Kaplan, R. R. Naik, N. Verma, F. G. Omenetto, M. C. McAlpine, *Nat. Commun.* **2012**, *3*, 763.

[13] D. Grieshaber, R. MacKenzie, J. Vörös, E. Reimhult, *Sensors* **2008**, *8*, 1400.

[14] J. Kim, J. R. Sempionatto, S. Imani, M. C. Hartel, A. Barfidokht, G. Tang, A. S. Campbell, P. P. Mercier, J. Wang, *Adv. Sci.* **2018**, *5*, 1800880.

[15] M. Lazaro, A. Lazaro, R. Villarino, D. Girbau, *Sensors* **2021**, *21*, 7472.

[16] J. Kim, S. Imani, W. R. de Araujo, J. Warchall, G. Valdés-Ramírez, T. R. Paixão, P. P. Mercier, J. Wang, *Biosens. Bioelectron.* **2015**, *74*, 1061.

[17] N. Thapliyal, T. E. Chiwunze, R. Karpoormath, R. N. Goyal, H. Patel, S. Cherukupalli, *RSC Adv.* **2016**, *6*, 57580.

[18] a) J. Heikenfeld, A. Jajack, J. Rogers, P. Gutruf, L. Tian, T. Pan, R. Li, M. Khine, J. Kim, J. Wang, *Lab Chip* **2018**, *18*, 217; b) H. Lee, T. K. Choi, Y. B. Lee, H. R. Cho, R. Ghaffari, L. Wang, H. J. Choi, T. D. Chung, N. Lu, T. Hyeon, S. H. Choi, D.-H. Kim, *Nat. Nanotechnol.* **2016**, *11*, 566; c) S. Zhuiykov, E. Kats, K. Kalantar-zadeh, M. Breedon, N. Miura, *Mater. Lett.* **2012**, *75*, 165; d) D. P. Rose, M. E. Ratterman, D. K. Griffin, L. Hou, N. Kelley-Loughnane, R. R. Naik, J. A. Hagen, I. Papautsky, J. C. Heikenfeld, *IEEE Trans. Biomed. Eng.* **2014**, *62*, 1457; e) S. Anastasova, B. Crewther, P. Bembnowicz, V. Curto, H. M. Ip, B. Rosa, G.-Z. Yang, *Biosens. Bioelectron.* **2017**, *93*, 139; f) S. Wang, Y. Wu, Y. Gu, T. Li, H. Luo, L.-H. Li, Y. Bai, L. Li, L. Liu, Y. Cao, *Anal. Chem.* **2017**, *89*, 10224.

[19] S. Assawajaruwan, B. Hitzmann, in *Encyclopedia of Analytical Science (Third Edition)* (Eds: P. Worsfold, C. Poole, A. Townshend, M. Miró), Elsevier, Amsterdam, The Netherlands, **2019**, Ch. Process Analysis | Bioprocess Analysis. https://doi.org/10.1016/B978-0-12-409547-2.11324-1.

[20] E. Sardini, M. Serpelloni, S. Tonello, *Biosensors* **2020**, *10*, 166.

[21] V. Haritha, S. S. Kumar, R. Rakhi, *Mater. Today: Proc.* **2022**, *50*, 34.

[22] J. L. Hammond, N. Formisano, P. Estrela, S. Carrara, J. Tkac, *Essays Biochem.* **2016**, *60*, 69.

[23] a) A. Curulli, *Molecules* **2021**, *26*, 2940; b) H. Ryu, D. Thompson, Y. Huang, B. Li, Y. Lei, *Sens. Actuators Rep.* **2020**, *2*, 100022.

[24] Y. Gao, L. Yu, J. C. Yeo, C. T. Lim, *Adv. Mater.* **2020**, *32*, 1902133.

[25] C. B. Frank, in *Clinical Methods: The History, Physical, and Laboratory Examinations* (3rd Edition) (Eds: H. K. Walker, W. D. Hall, J. W. Hurst), Butterworth, Boston, United States, **1990**, Ch. 114. https://www.ncbi.nlm.nih.gov/books/NBK218/.

[26] D. Harvey, N. W. Hayes, B. Tighe, *Contact Lens Anterior Eye* **2012**, *35*, 137.

[27] S. P. DiBartola, *Fluid, Electrolyte, and Acid-Base Disorders in Small Animal Practice*, Elsevier Health Sciences, Amsterdam **2011**.

[28] J. Kim, M. Kim, M.-S. Lee, K. Kim, S. Ji, Y.-T. Kim, J. Park, K. Na, K.-H. Bae, H. K. Kim, F. Bien, C. Y. Lee, J.-U. Park, *Nat. Commun.* **2017**, *8*, 14997.

[29] C. R. Taormina, J. T. Baca, S. A. Asher, J. J. Grabowski, D. N. Finegold, *J. Am. Soc. Mass Spectrom.* **2007**, *18*, 332.

[30] N. Thomas, I. Lähdesmäki, B. A. Parviz, *Sens. Actuators, B* **2012**, *162*, 128.

[31] Á. Farkas, R. Vámos, T. Bajor, N. Müllner, Á. Lázár, A. Hrabá, *Exp. Eye Res.* **2003**, *76*, 183.

[32] M. Park, H. Jung, Y. Jeong, K.-H. Jeong, *ACS Nano* **2017**, *11*, 438.

[33] A. Kijlstra, S. H. Jeurissen, K. M. Koning, *Br. J. Ophthalmol.* **1983**, *67*, 199.

[34] C. A. Paterson, M. C. O'Rourke, *Arch. Ophthalmol.* **1987**, *105*, 376.

[35] L. K. Banbury, Doctoral Thesis, Southern Cross University, **2009**. https://researchportal.scu.edu.au/esploro/outputs/doctoral/Stress-biomarkers-in-the-tear-film/991012821564402368.

[36] V. Andoralov, S. Shleev, T. Arnebrant, T. Ruzgas, *Anal. Bioanal. Chem.* **2013**, *405*, 3871.

[37] W.-M. Zhang, M. R. Natowicz, *Clin. Biochem.* **2013**, *46*, 694.

[38] V. Kumar, K. D. Gill, *Basic Concepts in Clinical Biochemistry: A Practical Guide*, Springer, Berlin **2018**.

[39] J. Zhao, H. Guo, J. Li, A. J. Bandodkar, J. A. Rogers, *Trends Chem.* **2019**, *1*, 559.

[40] S. Gupta, S. V. Sandhu, H. Bansal, D. Sharma, *J. Diabetes Sci. Technol.* **2015**, *9*, 91.

[41] A. J. Bandodkar, V. W. S. Hung, W. Jia, G. Valdés-Ramírez, J. R. Windmiller, A. G. Martinez, J. Ramírez, G. Chan, K. Kerman, J. Wang, *Analyst* **2013**, *138*, 123.

[42] W. Dang, L. Manjakkal, W. T. Navaraj, L. Lorenzelli, V. Vinciguerra, R. Dahiya, *Biosens. Bioelectron.* **2018**, *107*, 192.

[43] A. U. Alam, Y. Qin, S. Nambiar, J. T. Yeow, M. M. Howlader, N.-X. Hu, M. J. Deen, *Prog. Mater. Sci.* **2018**, *96*, 174.

[44] a) W. He, C. Wang, H. Wang, M. Jian, W. Lu, X. Liang, X. Zhang, F. Yang, Y. Zhang, *Sci. Adv.* **2019**, *5*, eaax0649; b) L. Mou, Y. Xia, X. Jiang, *Anal. Chem.* **2021**, *93*, 11525; c) H. Y. Y. Nyein, M. Bariya, L. Kivimäki, S. Uusitalo, T. S. Liaw, E. Jansson, C. H. Ahn, J. A. Hangasky, J. Zhao, Y. Lin, *Sci. Adv.* **2019**, *5*, eaaw9906; d) Q. Zhai, L. W. Yap, R. Wang, S. Gong, Z. Guo, Y. Liu, Q. Lyu, J. Wang, G. P. Simon, W. Cheng, *Anal. Chem.* **2020**, *92*, 4647; e) M. Parrilla, I. Ortiz-Gómez, R. Cánovas, A. Salinas-Castillo, M. Cuartero, G. n. A. Crespo, *Anal. Chem.* **2019**, *91*, 8644; f) W. Gao, S. Emaminejad, H. Y. Y. Nyein, S. Challa, K. Chen, A. Peck, H. M. Fahad, H. Ota, H. Shiraki, D. Kiriya, *Nature* **2016**, *529*, 509; g) M. Parrilla, M. Cuartero, S. P. Sánchez, M. Rajabi, N. Roxhed, F. Niklaus, G. Crespo, *Anal. Chem.* **2018**, *91*, 1578; h) Y. Tang, L. Zhong, W. Wang, Y. He, T. Han, L. Xu, X. Mo, Z. Liu, Y. Ma, Y. Bao, S. Gan, L. Niu, *Membranes* **2022**, *12*, 504.

[45] a) R. Burton, *The Mollusca-Physiology* **1983**, 293; b) I. Huhtaniemi, *Encyclopedia of Endocrine Diseases*, Elsevier Science, Amsterdam **2018**; c) A. Mathie, E. L. Veale, in *Encyclopedia of Neuroscience* (Eds: M. D. Binder, N. Hirokawa, U. Windhorst), Springer, Berlin, Heidelberg **2009**; d) B. Lu, Q. Zhang, H. Wang, Y. Wang, M. Nakayama, D. Ren, *Neuron* **2010**, *68*, 488.

[46] P. Mergenthaler, U. Lindauer, G. A. Dienel, A. Meisel, *Trends Neurosci.* **2013**, *36*, 587.

[47] B. Phypers, J. T. Pierce, *BJA Educ.* **2006**, *6*, 128.

[48] a) M. A. Djebbi, S. Boubakri, M. Braiek, N. Jaffrezic-Renault, P. Namour, A. B. H. Amara, *J. Electrochem. Soc.* **2021**, *168*, 057529; b) M. Thapa, R. Sung, Y. S. Heo, *Biosensors* **2021**, *11*, 507.

[49] Y. Yang, Y. Song, X. Bo, J. Min, O. S. Pak, L. Zhu, M. Wang, J. Tu, A. Kogan, H. Zhang, T. K. Hsiai, Z. Li, W. Gao, *Nat. Biotechnol.* **2020**, *38*, 217.

[50] H. Teymourian, A. Barfidokht, J. Wang, *Chem. Soc. Rev.* **2020**, *49*, 7671.

[51] K. Nagamine, T. Mano, A. Nomura, Y. Ichimura, R. Izawa, H. Furusawa, H. Matsui, D. Kumaki, S. Tokito, *Sci. Rep.* **2019**, *9*, 10102.

[52] X. Zhang, H. Ju, J. Wang, *Electrochemical Sensors, Biosensors and their Biomedical Applications*, Academic Press, Cambridge **2011**.

[53] W. Gao, X. Zhou, N. F. Heinig, J. P. Thomas, L. Zhang, K. T. Leung, *ACS Appl. Nano Mater.* **2021**, *4*, 4790.

[54] S. Neupane, S. Bhusal, V. Subedi, K. B. Nakarmi, D. K. Gupta, R. J. Yadav, A. P. Yadav, *J. Sens.* **2021**, *2021*, 8832748.

[55] a) Z.-P. Deng, Y. Sun, Y.-C. Wang, J.-D. Gao, *Sensors* **2018**, *18*, 3972; b) G. Matzeu, L. Florea, D. Diamond, *Sens. Actuators, B* **2015**, *211*, 403; c) K. M. Amin, F. Muench, U. Kunz, W. Ensinger, *J. Colloid Interface Sci.* **2021**, *591*, 384; d) D. Chu, F. Li, X. Song, H. Ma, L. Tan, H. Pang, X. Wang, D. Guo, B. Xiao, *J. Colloid Interface Sci.* **2020**, *568*, 130; e) J. Zhu, S. Liu, Z. Hu, X. Zhang, N. Yi, K. Tang, M. G. Dexheimer, X. Lian, Q. Wang, J. Yang, J. Gray, H. Cheng, *Biosens. Bioelectron.* **2021**, *193*, 113606.

[56] V. S. Reddy, B. Agarwal, Z. Ye, C. Zhang, K. Roy, A. Chinnappan, R. J. Narayan, S. Ramakrishna, R. Ghosh, *Nanomaterials* **2022**, *12*, 1082.

[57] T. Hibbard, A. J. Killard, *Crit. Rev. Anal. Chem.* **2011**, *41*, 21.

[58] B. Timmer, W. Olthuis, A. Van Den Berg, *Sens. Actuators, B* **2005**, *107*, 666.

[59] a) S. Nakata, T. Arie, S. Akita, K. Takei, *ACS Sens.* **2017**, *2*, 443; b) M. H. Fakir, J. K. Kim, *Build. Environ.* **2022**, *207*, 108507; c) H. Lee, C. Song, Y. S. Hong, M. Kim, H. R. Cho, T. Kang, K. Shin, S. H. Choi, T. Hyeon, D.-H. Kim, *Sci. Adv.* **2017**, *3*, e1601314.

[60] a) N. M. Farandos, A. K. Yetisen, M. J. Monteiro, C. R. Lowe, S. H. Yun, *Adv. Healthcare Mater.* **2015**, *4*, 792; b) A. J. Bandodkar, J. Wang, *Trends Biotechnol.* **2014**, *32*, 363.

[61] M. Elsherif, R. Moreddu, F. Alam, A. E. Salih, I. Ahmed, H. Butt, *Front. Med.* **2022**, *9*, 858784.

[62] H. Yao, A. J. Shum, M. Cowan, I. Lähdesmäki, B. A. Parviz, *Biosens. Bioelectron.* **2011**, *26*, 3290.

[63] D. H. Keum, S.-K. Kim, J. Koo, G.-H. Lee, C. Jeon, J. W. Mok, B. H. Mun, K. J. Lee, E. Kamrani, C.-K. Joo, S. Shin, J.-Y. Sim, D. Myung, S. H. Yun, Z. Bao, S. K. Hahn, *Sci. Adv.* **2020**, *6*, eaba3252.

[64] Y.-R. Lin, C.-C. Hung, H.-Y. Chiu, P.-H. Chang, B.-R. Li, S.-J. Cheng, J.-W. Yang, S.-F. Lin, G.-Y. Chen, *Sensors* **2018**, *18*, 3208.

[65] S. Mondal, S. Karuppuswami, R. Steinhorst, P. Chahal, presented at *2019 IEEE 69th Electronic Components and Technology Conference (ECTC)*, **2019**.

[66] L. García-Carmona, A. Martín, J. R. Sempionatto, J. R. Moreto, M. C. González, J. Wang, A. Escarpa, *Anal. Chem.* **2019**, *91*, 13883.

[67] T. Arakawa, Y. Kuroki, H. Nitta, P. Chouhan, K. Toma, S.-i. Sawada, S. Takeuchi, T. Sekita, K. Akiyoshi, S. Minakuchi, K. Mitsubayashi, *Biosens. Bioelectron.* **2016**, *84*, 106.

[68] T. Arakawa, K. Tomoto, H. Nitta, K. Toma, S. Takeuchi, T. Sekita, S. Minakuchi, K. Mitsubayashi, *Anal. Chem.* **2020**, *92*, 12201.

[69] J. Kim, S. Imani, W. R. de Araujo, J. Warchall, G. Valdés-Ramírez, T. R. L. C. Paixão, P. P. Mercier, J. Wang, *Biosens. Bioelectron.* **2015**, *74*, 1061.

[70] M. Soukup, I. Biesiada, A. Henderson, B. Idowu, D. Rodeback, L. Ridpath, E. G. Bridges, A. M. Nazar, K. G. Bridges, *Diabetol. Metab. Syndr.* **2012**, *4*, 14.

[71] R. Sha, L. Durai, S. Badhulika, presented at *2018 4th IEEE International Conference on Emerging Electronics (ICEE)*, Bengaluru, India, December 2018, https://ieeexplore.ieee.org/document/8937860.

[72] R. Zou, S. Shan, L. Huang, Z. Chen, T. Lawson, M. Lin, L. Yan, Y. Liu, *ACS Biomater. Sci. Eng.* **2020**, *6*, 673.

[73] J. Park, J. Kim, S.-Y. Kim, W. H. Cheong, J. Jang, Y.-G. Park, K. Na, Y.-T. Kim, J. H. Heo, C. Y. Lee, *Sci. Adv.* **2018**, *4*, eaap9841.

[74] C. Xiong, T. Zhang, W. Kong, Z. Zhang, H. Qu, W. Chen, Y. Wang, L. Luo, L. Zheng, *Biosens. Bioelectron.* **2018**, *101*, 21.

[75] a) C. Yáñez, G. DeMas-Giménez, S. Royo, *Sensors* **2022**, *22*, 6836; b) K. S. Maiti, M. Lewton, E. Fill, A. Apolonski, *Sci. Rep.* **2019**, *9*, 16167; c) K. S. Maiti, S. Roy, R. Lampe, A. Apolonski, *J. Biophotonics* **2020**, *13*, e202000125; d) J. D. Pleil, *Arch. Toxicol.* **2016**, *90*, 2669; e) P. M.-L. Sinues, M. Kohler, R. Zenobi, *PLoS One* **2013**, *8*, e59909.

[76] A. H. Jalal, F. Alam, S. Roychoudhury, Y. Umasankar, N. Pala, S. Bhansali, *ACS Sens.* **2018**, *3*, 1246.

[77] W. Hu, W. Wu, Y. Jian, H. Haick, G. Zhang, Y. Qian, M. Yuan, M. Yao, *Nano Res.* **2022**, *15*, 8185.

[78] A. T. Güntner, S. Abegg, K. Königstein, P. A. Gerber, A. Schmidt-Trucksäss, S. E. Pratsinis, *ACS Sens.* **2019**, *4*, 268.

[79] E. Bihar, Y. Deng, T. Miyake, M. Saadaoui, G. G. Malliaras, M. Rolandi, *Sci. Rep.* **2016**, *6*, 27582.

[80] J. L. Tan, Z. X. Yong, C. K. Liam, *J. Thorac. Dis.* **2016**, *8*, 2772.

[81] T. Sarkar, S. Srinives, A. Rodriquez, A. Mulchandani, *Electroanalysis* **2018**, *30*, 2077.

[82] P. Ma, J. Li, Y. Chen, B. A. Z. Montano, H. Luo, D. Zhang, H. Zheng, Y. Liu, H. Lin, W. Zhu, G. Zhang, H. Mao, J. Yu, Z. Chen, *Microw Opt. Technol. Lett.* **2021**, https://doi.org/10.1002/mop.33133.

[83] S. W. Ryter, A. M. Choi, *J. Breath Res.* **2013**, *7*, 017111.

[84] C. M. Issarow, N. Mulder, R. Wood, *J. Theor. Biol.* **2015**, *372*, 100.

[85] T. Hibbard, K. Crowley, F. Kelly, F. Ward, J. Holian, A. Watson, A. J. Killard, *Anal. Chem.* **2013**, *85*, 12158.

[86] F. Güder, A. Ainla, J. Redston, B. Mosadegh, A. Glavan, T. J. Martin, G. M. Whitesides, *Angew. Chem., Int. Ed.* **2016**, *55*, 5727.

[87] L. Ma, R. Wu, H. Miao, X. Fan, L. Kong, A. Patil, X. Y. Liu, J. Wang, *Text. Res. J.* **2021**, *91*, 398.

[88] A. T. Güntner, N. J. Pineau, D. Chie, F. Krumeich, S. E. Pratsinis, *J. Mater. Chem. B* **2016**, *4*, 5358.

[89] A. Gholizadeh, D. Voiry, C. Weisel, A. Gow, R. Laumbach, H. Kipen, M. Chhowalla, M. Javanmard, *Microsyst. Nanoeng.* **2017**, *3*, 17022.

[90] N. U. Nazir, S. R. Abbas, H. Nasir, I. Hussain, *J. Electroanal. Chem.* **2022**, *905*, 115977.

[91] a) J. Suo, Y. Liu, C. Wu, M. Chen, Q. Huang, Y. Liu, K. Yao, Y. Chen, Q. Pan, X. Chang, A. Y. L. Leung, H.-y. Chan, G. Zhang, Z. Yang, W. Daoud, X. Li, V. A. L. Roy, J. Shen, X. Yu, J. Wang, W. J. Li, *Adv. Sci.* **2022**, *9*, 2203565; b) P. Escobedo, M. D. Fernández-Ramos, N. López-Ruiz, O. Moyano-Rodríguez, A. Martínez-Olmos, I. M. P. d. Vargas-Sansalvador, M. A. Carvajal, L. F. Capitán-Vallvey, A. J. Palma, *Nat. Commun.* **2022**, *13*, 72; c) P. Lee, H. Kim, Y. Kim, W. Choi, M. S. Zitouni, A. Khandoker, H. F. Jelinek, L. Hadjileontiadis, U. Lee, Y. Jeong, *JMIR Mhealth Uhealth* **2022**, *10*, e38614.
[92] I. Jeerapan, W. Sangsudcha, P. Phokhonwong, *Sens. Biosens. Res.* **2022**, *38*, 100525.
[93] K. Roberts, A. Jaffe, C. Verge, P. S. Thomas, *J. Diabetes Sci. Technol.* **2012**, *6*, 659.
[94] S. I. Hwang, H.-Y. Chen, C. Fenk, M. A. Rothfuss, K. N. Bocan, N. G. Franconi, G. J. Morgan, D. L. White, S. C. Burkert, J. E. Ellis, M. L. Vinay, D. A. Rometo, D. N. Finegold, E. Sejdic, S. K. Cho, A. Star, *ACS Sens.* **2021**, *6*, 871.
[95] J. Zhang, J. Liu, H. Su, F. Sun, Z. Lu, A. Su, *Sens. Actuators, B* **2021**, *341*, 130046.
[96] H. Su, F. Sun, Z. Lu, J. Zhang, W. Zhang, J. Liu, *Sens. Actuators, B* **2022**, *357*, 131459.
[97] X. Li, C. Zhan, Q. Huang, M. He, C. Yang, C. Yang, X. Huang, M. Chen, X. Xie, H.-J. Chen, *ACS Appl. Nano Mater.* **2022**, *5*, 4767.
[98] F. Ghaderinezhad, H. C. Koydemir, D. Tseng, D. Karinca, K. Liang, A. Ozcan, S. Tasoglu, *Sci. Rep.* **2020**, *10*, 13620.
[99] a) I. Brook, A. B. Belman, G. Controni, *Am. J. Clin. Pathol.* **1981**, *75*, 110; b) H. Bartels, W. Berger, *Intensive Care Med.* **1980**, *6*, 235; c) X. Li, Y. Yang, B. Zhang, X. Lin, X. Fu, Y. An, Y. Zou, J.-X. Wang, Z. Wang, T. Yu, *Signal Transduction Targeted Ther.* **2022**, *7*, 305.
[100] C. Rose, A. Parker, B. Jefferson, E. Cartmell, *Crit. Rev. Environ. Sci. Technol.* **2015**, *45*, 1827.
[101] M. N. P. Liman, I. Jialal, *Physiology,Glycosuria*, StatPearls Publishing, Treasure Island, FL **2022**.
[102] X. Ding, Y. Zhang, Y. Zhang, X. Ding, H. Zhang, T. Cao, Z.-b. Qu, J. Ren, L. Li, Z. Guo, F. Xu, Q.-X. Wang, X. Wu, G. Shi, H. Haick, M. Zhang, *ACS Nano* **2022**, *16*, 17376.
[103] Y. Jian, N. Zhang, T. Liu, Y. Zhu, D. Wang, H. Dong, L. Guo, D. Qu, X. Jiang, T. Du, Y. Zheng, M. Yuan, X. Fu, J. Liu, W. Dou, F. Niu, R. Ning, G. Zhang, J. Fan, H. Haick, W. Wu, *ACS Sens.* **2022**, *7*, 1720.
[104] M. Arivazhagan, A. Shankar, G. Maduraiveeran, *Microchim. Acta* **2020**, *187*, 468.
[105] M. Arivazhagan, G. Maduraiveeran, *J. Electroanal. Chem.* **2020**, *874*, 114465.
[106] A. Go, S. R. Park, Y. Ku, M. Sun, S. Yeon, J. K. Lee, S. W. Lee, M. H. Lee, *Sensors* **2021**, *21*, 4902.
[107] S. Karastogianni, I. Paraschi, S. Girousi, *Biosens. Bioelectron.: X* **2022**, *12*, 100275.
[108] N. Manjula, S. Pulikkutty, S.-M. Chen, *Colloids Surf. A* **2023**, *660*, 130830.
[109] N. F. Atta, A. Galal, D. M. El-Said, *ACS Omega* **2019**, *4*, 17947.
[110] M. Bariya, H. Y. Y. Nyein, A. Javey, *Nat. Electron.* **2018**, *1*, 160.
[111] J. Kim, W. R. de Araujo, I. A. Samek, A. J. Bandodkar, W. Jia, B. Brunetti, T. R. L. C. Paixão, J. Wang, *Electrochem. Commun.* **2015**, *51*, 41.
[112] H. Y. Y. Nyein, M. Bariya, B. Tran, C. H. Ahn, B. J. Brown, W. Ji, N. Davis, A. Javey, *Nat. Commun.* **2021**, *12*, 1823.
[113] S. Emaminejad, W. Gao, E. Wu, Z. A. Davies, H. Yin Yin Nyein, S. Challa, S. P. Ryan, H. M. Fahad, K. Chen, Z. Shahpar, *Proc. Natl. Acad. Sci. U. S. A.* **2017**, *114*, 4625.
[114] M. J. Patterson, S. D. Galloway, M. A. Nimmo, *Exp. Physiol.* **2000**, *85*, 869.
[115] A. Abellán-Llobregat, I. Jeerapan, A. Bandodkar, L. Vidal, A. Canals, J. Wang, E. Morallon, *Biosens. Bioelectron.* **2017**, *91*, 885.
[116] J. R. Windmiller, A. J. Bandodkar, G. Valdés-Ramírez, S. Parkhomovsky, A. G. Martinez, J. Wang, *Chem. Commun.* **2012**, *48*, 6794.
[117] J. Kim, I. Jeerapan, S. Imani, T. N. Cho, A. Bandodkar, S. Cinti, P. P. Mercier, J. Wang, *ACS Sens.* **2016**, *1*, 1011.
[118] D. Kinnamon, R. Ghanta, K.-C. Lin, S. Muthukumar, S. Prasad, *Sci. Rep.* **2017**, *7*, 13312.
[119] Y. Y. Broza, X. Zhou, M. Yuan, D. Qu, Y. Zheng, R. Vishinkin, M. Khatib, W. Wu, H. Haick, *Chem. Rev.* **2019**, *119*, 11761.
[120] C. J. Harvey, R. F. LeBouf, A. B. Stefaniak, *Toxicol. In Vitro* **2010**, *24*, 1790.
[121] Y. Wang, X. Wang, W. Lu, Q. Yuan, Y. Zheng, B. Yao, *Talanta* **2019**, *198*, 86.
[122] X. Luo, L. Guo, Y. Liu, W. Shi, W. Gai, Y. Cui, *IEEE Sens. J.* **2019**, *20*, 3757.
[123] L. Wang, M. Xu, Y. Xie, C. Qian, W. Ma, L. Wang, Y. Song, *Sens. Actuators, B* **2019**, *285*, 264.
[124] A. Weremfo, S. T. C. Fong, A. Khan, D. B. Hibbert, C. Zhao, *Electrochim. Acta* **2017**, *231*, 20.
[125] F. Y. Lin, P. Y. Lee, T. F. Chu, C. I. Peng, G. J. Wang, *Int. J. Nanomed.* **2021**, *16*, 5551.
[126] A. Abellán-Llobregat, I. Jeerapan, A. Bandodkar, L. Vidal, A. Canals, J. Wang, E. Morallón, *Biosens. Bioelectron.* **2017**, *91*, 885.
[127] H. Yoon, J. Nah, H. Kim, S. Ko, M. Sharifuzzaman, S. C. Barman, X. Xuan, J. Kim, J. Y. Park, *Sens. Actuators, B* **2020**, *311*, 127866.
[128] F. Alam, A. H. Jalal, S. Forouzanfar, M. Karabiyik, A. R. Baboukani, N. Pala, *IEEE Sens. J.* **2020**, *20*, 5102.
[129] S. M. Mugo, J. Alberkant, *IEEE Sens. J.* **2020**, *20*, 5741.
[130] K. C. Lin, S. Muthukumar, S. Prasad, *Talanta* **2020**, *214*, 120810.
[131] V. Mazzaracchio, A. Serani, L. Fiore, D. Moscone, F. Arduini, *Electrochim. Acta* **2021**, *394*, 139050.
[132] P. Pirovano, M. Dorrian, A. Shinde, A. Donohoe, A. J. Brady, N. M. Moyna, G. Wallace, D. Diamond, M. McCaul, *Talanta* **2020**, *219*, 121145.
[133] A. Ganguly, S. Prasad, *Sensors* **2019**, *19*, 4590.
[134] L. Manjakkal, W. Dang, N. Yogeswaran, R. Dahiya, *Biosensors* **2019**, *9*, 14.
[135] M. Gamella, S. Campuzano, J. Manso, G. G. de Rivera, F. López-Colino, A. Reviejo, J. Pingarrón, *Anal. Chim. Acta* **2014**, *806*, 1.
[136] J. Biscay, E. Findlay, L. Dennany, *Talanta* **2021**, *224*, 121815.
[137] J. Yoon, M. Sim, T.-S. Oh, Y. S. Yoon, D.-J. Kim, *J. Electrochem. Soc.* **2021**, *168*, 117510.
[138] S. Madhu, A. J. Anthuuvan, S. Ramasamy, P. Manickam, S. Bhansali, P. Nagamony, V. Chinnuswamy, *ACS Appl. Electron. Mater.* **2020**, *2*, 499.
[139] F. Poletti, B. Zanfrognini, L. Favaretto, V. Quintano, J. Sun, E. Treossi, M. Melucci, V. Palermo, C. Zanardi, *Sens. Actuators, B* **2021**, *344*, 130253.

Jimin Lee is currently a Postdoctoral Research Fellow in the George W. Woodruff School of Mechanical Engineering at Georgia Institute of Technology. She received her B.S. in chemical engineering from Hanyang University (Republic of Korea) in 2015, and Ph.D. in Materials Science and Chemical Engineering from Hanyang University in 2021. Her research interests lie in wearable flexible sensors, electrochemical sensors, biosensors, and nanomaterial interfaces.

Myung Chul Kim is an Undergraduate Student in the department of Mechanical Engineering at Korea Advanced Institute of Science and Technology (KAIST), Republic of Korea. His research interests involve mechanics of materials/structures, vibrations, acoustics, mechanobiology, and soft electronics.

Ira Soltis is currently a Graduate Student and Research Assistant in George W. Woodruff School of Mechanical Engineering at Georgia Institute of Technology. He received his B.S. in Mechanical Engineering from Georgia Institute of Technology in 2020. His research interests include wearable robotics, such as pneumatic soft actuator-based exoskeleton robots.

Sung Hoon Lee is a Graduate Research Assistant, pursuing Ph.D., in the Electrical and Computer Engineering department at Georgia Institute of Technology. He received his B.S. in Electrical Engineering from the University of Illinois at Urbana-Champaign. His research areas include wearable electronics, embedded systems design, and signal processing.

Woon-Hong Yeo is a Woodruff Faculty Fellow, Associate Professor in the Mechanical Engineering and Biomedical Engineering, and the Director of the IEN Center for Human-Centric Interfaces and Engineering at Georgia Institute of Technology. Dr. Yeo received his Ph.D. in Mechanical Engineering at the University of Washington, Seattle in 2011. From 2011 to 2013, he worked as a Postdoctoral Research Fellow at the University of Illinois at Urbana-Champaign. Dr. Yeo has published over 130 peer-reviewed research articles. His research focuses on the areas of nano-/microengineering, advanced soft materials, molecular interactions, and bio-electromechanical systems, with an emphasis on stretchable hybrid electronics.